

DESTRUCTION OF TOLUENE
IN A DIELECTRIC BARRIER
DISCHARGE PLASMA
REACTOR

By

ELANGO VAN KARUPPASAMY

Bachelor of Science

University of Madras

Chennai, India

2002

Submitted to the Faculty of the
Graduate College of the
Oklahoma State University
in partial fulfillment of
the requirements for
the Degree of
MASTER OF SCIENCE
December 2004

DESTRUCTION OF TOLUENE
IN A DIELECTRIC BARRIER
DISCHARGE PLASMA
REACTOR

Thesis Approved:

Dr. John N. Veenstra

Thesis Adviser

Dr. Gregory Wilber

Dr. A. H. Johannas

Dr. A. Gordon Emslie

Dean of the Graduate College

ACKNOWLEDGMENTS

I wish to express my sincere appreciation to my major Dr. John N. Veenstra for his constructive guidance, assistance, and intelligent supervision throughout this research and my masters program. I also deeply appreciate other committee members, Dr. A. H. Johannas and Dr. Gregory Wilber for their invaluable help to this research.

Moreover I express my thanks to Dr. Sanders for her support throughout my masters program. I also deeply express my sincere thanks to Dr. Greg Holland for his help throughout this research.

Finally I am deeply indebted to my parents Karuppasamy and Thamizharasi, my sister Thamariselvi for their support and love during my studies abroad in the United States. And special thanks to Annu for her encouragement throughout my studies. I would also like to thank all my friends especially to Sundarraja Mani, Addy and Kalpathy Vijay for their support to complete this thesis.

Table of Contents

| Chapter | Page |
|--|------|
| 1. Introduction | 1 |
| 2. Literature Review | 3 |
| 2.1 Plasma | 3 |
| 2.2 Alternating Current Plasma | 5 |
| 2.3 Properties of Toluene | 8 |
| 2.4 Alternating Methods of Toluene destruction | 8 |
| 2.5 Corona Chemistry of Toluene | 10 |
| 2.6 Destruction Studies of Toluene | 12 |
| 3. Methods and Materials | 14 |
| 3.1 Experimental Setup | 14 |
| 3.1.1. Reactor System | 14 |
| 3.1.2. Electrical System | 17 |
| 3.1.3. Plumbing System | 22 |
| 3.1.4. Analysis System | 28 |
| 3.2 Experimental Design | 33 |
| 3.2.1. Secondary Voltage Variation | 33 |
| 3.2.2. Frequency Variation | 35 |
| 3.2.3. Flow Rate Variation | 35 |
| 3.2.4. Energy Density Variation | 36 |
| 3.2.5. Detection of Byproducts | 36 |
| 3.2.6. Carbon Balance | 36 |

| Chapter | Page |
|--|-------------|
| 4. Results and Discussions | 38 |
| 4.1 Calibration Data for the Plasma Reactor | 38 |
| 4.2 Effect of Secondary Voltage on Destruction | 40 |
| 4.3 Effect of Frequency on Destruction | 43 |
| 4.4 Effect of Flow Rate on Destruction | 46 |
| 4.5 Effect of Energy Density on Destruction | 48 |
| 4.6 Carbon Balance | 53 |
| 4.7 Repeatability | 54 |
| 4.8 Cost Analysis | 55 |
| 5. Conclusions and Recommendations | 57 |
| 5.1 Conclusions | 59 |
| 5.2. Recommendations | 61 |
| Bibliography | 62 |
| Appendices | |
| Appendix A | 65 |
| Appendix B | 67 |
| Appendix C | 71 |
| Appendix D | 73 |
| Appendix E | 76 |
| Appendix F | 78 |
| Appendix G | 80 |
| Appendix H | 83 |
| Appendix I | 86 |
| Appendix J | 88 |
| Appendix K | 91 |
| Appendix L | 93 |

List of Tables

| Table | Page |
|--|-------------|
| 1. Scale up Parameter, β for Various Compounds | 13 |
| 2. Matrix of Runs | 34 |
| 3. Effect of Secondary Voltage on Destruction of Toluene | 41 |
| 4. Effect of Frequency on Destruction of Toluene | 43 |
| 5. Effect of Flow Rate on Destruction of Toluene | 46 |
| 6. Effect of Energy Density on Destruction of Toluene | 49 |
| 7. Carbon Balance of Toluene | 55 |
| 8. Capital Cost | 58 |

List of Figures

| Figure | Page |
|--|-------------|
| 1. States of Matter | 4 |
| 2. Plasma Temperature and Densities | 5 |
| 3. Dielectric Barrier Discharge | 7 |
| 4. Total Annual Cost Comparison of Compounds at 20,000 cfm and 2000 ppm | 9 |
| 5. Removal Cost per Unit Contaminant at 20,000 cfm and 2000 ppm | 10 |
| 6. Dimensions of Single Tube Single Dielectric Reactor | 15 |
| 7. Single Tube Single Dielectric Reactor | 16 |
| 8. Electrical System | 17 |
| 9. Oscillator | 18 |
| 10. Transformer | 19 |
| 11. Voltage and Current Measuring Circuit | 20 |
| 12. Secondary Power Source | 21 |
| 13. Data Acquisition Board | 21 |
| 14. Plumbing System | 23 |
| 15. Mass Flow Controller | 24 |
| 16. Mass Flow Controller Panel | 24 |
| 17. Syringe Pump | 25 |
| 18. Thermostat | 26 |
| 19. Gas Chromatograph Unit | 27 |

| Figure | Page |
|--|-------------|
| 20. Methanizer | 37 |
| 21. Toluene Calibration Curve | 39 |
| 22. CO Calibration Curve | 39 |
| 23. CO ₂ Calibration Curve | 40 |
| 24. Destruction Run at 15000 Secondary Voltage | 41 |
| 25. Destruction Run at 12000 Secondary Voltage | 42 |
| 26. Destruction Run at 9000 Secondary Voltage | 42 |
| 27. Destruction Run at 200 Hz Frequency | 44 |
| 28. Destruction Run at 250 Hz Frequency | 44 |
| 29. Destruction Run at 300 Hz Frequency | 45 |
| 30. Destruction Run at 6 ml/s of Flow Rate | 46 |
| 31. Destruction Run at 8 ml/s of Flow Rate | 47 |
| 32. Destruction Run at 10 ml/s of Flow Rate | 47 |
| 33. Destruction Run at 1397 J/l Energy Density | 49 |
| 34. Destruction Run at 2168 J/l Energy Density | 50 |
| 35. Destruction Run at 3333 J/l Energy Density | 50 |
| 36. Destruction Run at 3873 J/l Energy Density | 51 |
| 37. Destruction Run at 4210 J/l Energy Density | 51 |
| 38. Destruction Run at 6423 J/l Energy Density | 52 |
| 39. Destruction Run at 7093 J/l Energy Density | 52 |
| 40. Scale up factor Calculation for Toluene | 53 |
| 41. DRE vs. Energy Density | 53 |

| | |
|---|----|
| 42. Carbon Balance of Run 1 | 55 |
| 43. Repeatability of Run 16 and Duplicate | 56 |

1. Introduction

National Emission Standards for Hazardous Air Pollutants for the Aerospace Manufacturing and Rework Facilities Source Category are set out by Congress in the Title 40 Code of Federal Regulations (40 CFR 63.741). The Oklahoma City Air Logistics Center (OC-ALC) at Tinker Air Force Base (TAFB) conducts surface coating in its paint booths as part of the maintenance activities conducted at the facility. Air exhaust from the OC-ALC paint booths contain a variety of Volatile Organic Compounds (VOCs) that serve as solvents in the paint. Typical VOCs contained in the paint booths at TAFB are shown in Appendix A. The Clean Air Act Amendments of 1990 required the Environmental Protection Agency to establish more stringent emission standards for 189 Hazardous Air Pollutants (HAPs) that are related with approximately 300 major source categories (Pytte, 1990). Most of the HAPs listed are volatile organic compounds like toluene, butanol and butyl acetate. These contaminants are known for their adverse effects on human health and persistence in the atmosphere. HAPs need to be controlled according to Maximum Achievable Control Technology (MACT) standards (Agnihotri, 2003). Conventional MACT for removing VOCs from air streams include condensation, incineration, absorption, and adsorption processes with an average control efficiency of 90%. Depending on the source of contaminants, the concentrations of VOCs in the resulting gas streams may vary from very low values (tens of ppbv) to very high values (few percent by volume), which can render some of the control technologies ineffective for certain pollutant concentrations (Agnihotri, 2003). Carbon adsorption has fire potential in the carbon bed when high concentrations of ketone and alcohol are present (Unit Cost Estimator, 2003). In view of the constraints of existing control technologies,

it would be highly desirable to have a control technology capable of effectively and efficiently removing multiple gas-phase pollutants present in varying concentrations.

Further, the painting operations common at TAFB are not continuous but are of short duration. Due to this pattern of emissions generation, a technology with an “instant-on”/ “instant off” capability would be the most efficient type of treatment for use by TAFB. TAFB has commissioned the investigation of an innovative technology to attempt to meet the 90% removal efficiency of an acceptable removal technology with a process that is better adapted to the conditions and scheduling of the paint booths. A Dielectric Barrier Discharge (DBD) plasma reactor is an innovative technology developed at Oklahoma State University that is known to destroy some of the compounds of interest as well as having an “instant-on”/ “instant-off” capability.

This research investigated the feasibility of a single tube single DBD plasma reactor with an instant-on and instant-off capability for the destruction of contaminants and to calculate a scale-up parameter, β . This scale up parameter gives the relationship between destruction efficiency and energy density (power/flow rate) of the compounds. In order to achieve these goals, toluene was selected for this research due to its relative high volatility from the paint booth emissions. The scale up parameter is calculated by keeping the inlet concentration and relative humidity constant and changing the secondary voltage, flow rate, and/or frequency.

2. Literature Review

While studying the destruction of toluene in a dielectric barrier discharge plasma reactor, the aspects that require further study are: 1) Plasma, Alternating Current Plasma 2) Properties of toluene, Corona chemistry of toluene, Alternative methods of toluene destruction, and 3) Destruction studies of toluene. To gain a sound knowledge on the above-mentioned aspects a literature survey was conducted. The result of this survey are detailed in the succeeding paragraphs.

2.1. Plasma

The different states of matter generally found on earth are solid, liquid, and gas. Sir William Crookes, an English physicist, identified a fourth state of matter, now called plasma, in 1879 (Plasma Science, 2003). “The word "PLASMA" was first applied to ionized gas by Dr. Irving Langmuir, an American chemist and physicist, in 1929” (Plasma Science, 2003). Figure 1 gives the various states of matter.




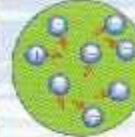
| Solid | Liquid | Gas | Plasma |
|---|---|---|--|
| Example Ice H_2O | Example Water H_2O | Example Steam H_2O | Example Ionized Gas $H_2 \rightarrow H^+ + H^+ + 2e^-$ |
| Cold $T < 0^\circ C$ | Warm $0 < T < 100^\circ C$ | Hot $T > 100^\circ C$ | Hotter $T > 100,000^\circ C$ (> 10 electron Volts) |
|  |  |  |  |
| Molecules Fixed in Lattice | Molecules Free to Move | Molecules Free to Move, Large Spacing | Ions and Electrons Move Independently, Large Spacing |

Figure 1: States of Matter (Plasma Science, 2003)

From Figure 1 it is seen that plasmas are conductive assemblies of charged particles.

Further, plasmas are the most common form of matter comprising more than 99% of the visible universe. (Plasma Science, 2003)

The graph given below (Figure 2) shows where many types of plasma can occur in terms of number density and temperatures conditions (Plasma Science, 2003). But the full range of plasmas can go beyond this illustration.

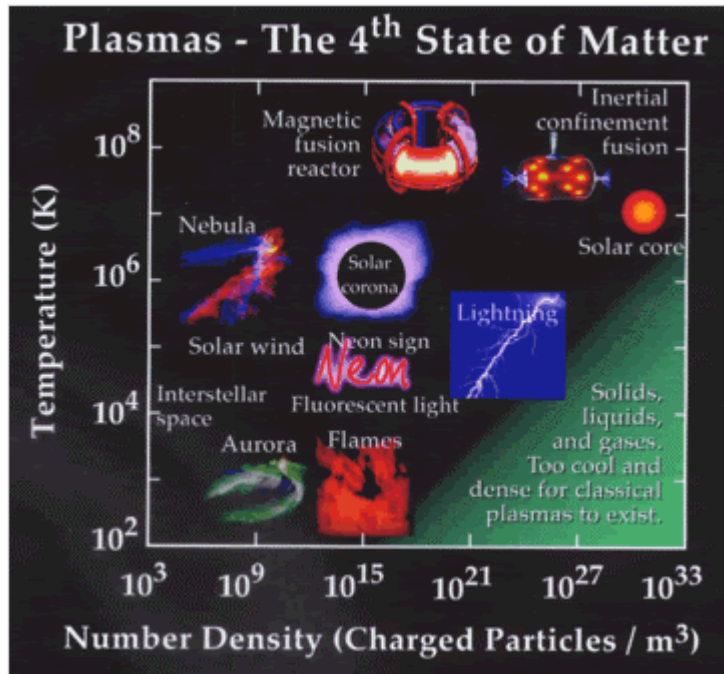


Figure 2: Plasma Temperature and Densities.

2.2. Alternating Current Plasma

Plasmas can appear in such forms as heat-induced, radiation-induced, and electrically induced plasmas. The plasma forms due to the acceleration of electrons independently of the particles around them. Inside a plasma formation several reactions (Glockler, 1939) take place including:

- Rebound,
- Radical formation,
- Higher orbital electron clusters, and
- Light production.

The application of plasma as a gas-phase oxidation processes that can destroy air pollutants is a relatively recent process. "It is an extensively studied advanced oxidation technology (AOT) that envisions production of highly reactive gas-phase free radicals,

such as $\cdot\text{O}$ (^3P) and $\cdot\text{OH}$ that can initiate and sustain a complex chemistry of pollutant destruction reactions” (Agnihotri, 2003). It is often produced by creating electrical discharges in a dielectric barrier electrode arrangement (commonly known as DBD or Single Dielectric Plasma (SDP) reactor) and is referred to as the discharge occurring in the open space between either one or two insulated electrodes (Figure 3) connected to a source of high voltage alternating current. The geometry of such reactors is either planar or cylindrical with a configuration similar to that of a parallel-plate or a cylindrical capacitor, respectively (Veenstra, 2003). Usually, one or both metal electrodes are covered with a dielectric material (Pyrex, quartz, ceramic etc.) that separates them from a thin gas layer. The presence of a dielectric splits the electrical discharges into numerous micro discharges of high instantaneous current and spatially distributes them over the discharge area and, hence, increases the homogeneity of plasma reactors (Rosocha, 1996).

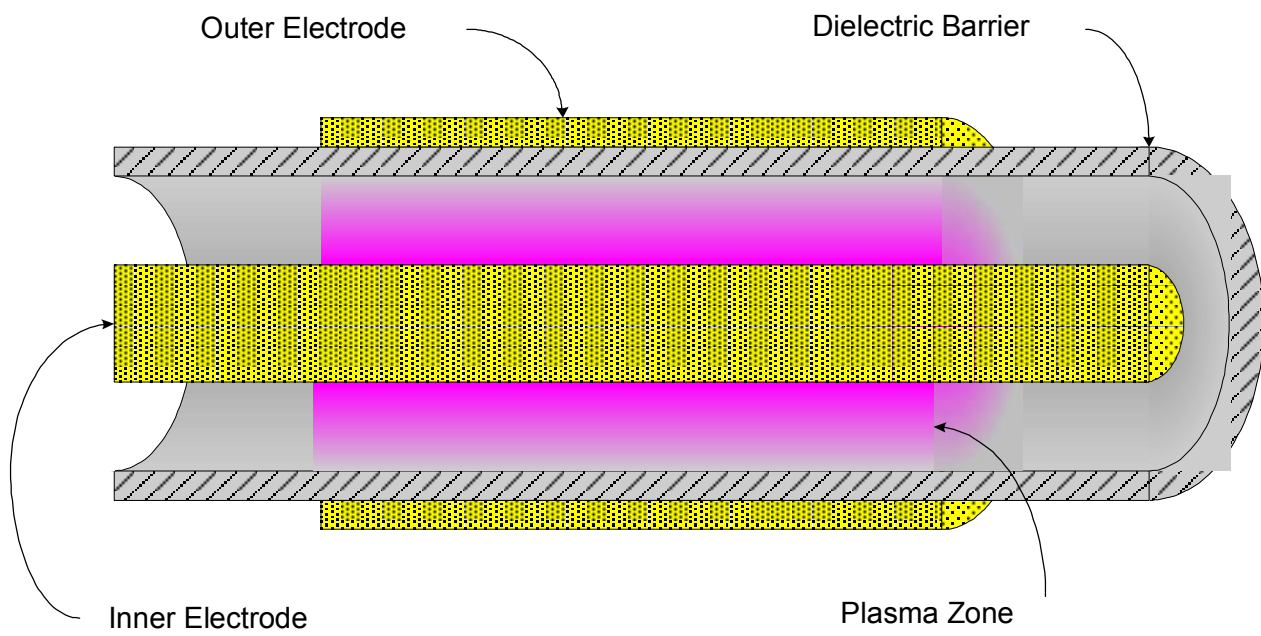


Figure 3: Dielectric Barrier Discharge (Veenstra, 2003)

2.3. Properties of Toluene

Toluene

Toluene is a clear, colorless liquid with an aromatic benzene-like odor. It has a specific gravity of 0.86 at 20 °C and is has a solubility of 0.05 gm/100gm water at 20 °C (68 ° F) in water. It has a boiling point of 111 °C (232 ° F), melting point of -95 °C (-139 ° F), vapor pressure of 22 mm Hg at 20 °C (68 ° F), vapor density of 3.14, and an evaporation rate of 2.24 (SIRI MSDS, 2003).

Environmental Toxicity:

The LC50/96-hour values for fish are between 10 and 100 mg/l (SIRI MSDS, 2003).

In human beings the primary effect is on the central nervous system. Single short-term exposure toluene (750 mg/m³ for 8 hours) has reportedly caused transient eye and respiratory irritation. Repeated long-term exposure in this range can cause neurological damage (WHO, 1985).

2.4. Alternative Methods of Toluene Destruction

Toluene can be removed by adsorption using activated carbon, thermal oxidation and incineration, bio-filtration and plasma destruction (Veenstra, 2003).

Carbon adsorption is cheap and effective (90%) compared with other methods but the presence of high concentrations of ketones and alcohols can causes fire in a carbon bed (Unit Cost Estimator, 2003).

Finally, the destruction VOCs using an alternate current plasma reactor is effective (>95% Destruction Efficiency) and potentially less expensive than other

competing technologies. The following Figures (4 and 5), give a better view of the cost of various control technologies (Unit Cost Estimator, 2003).

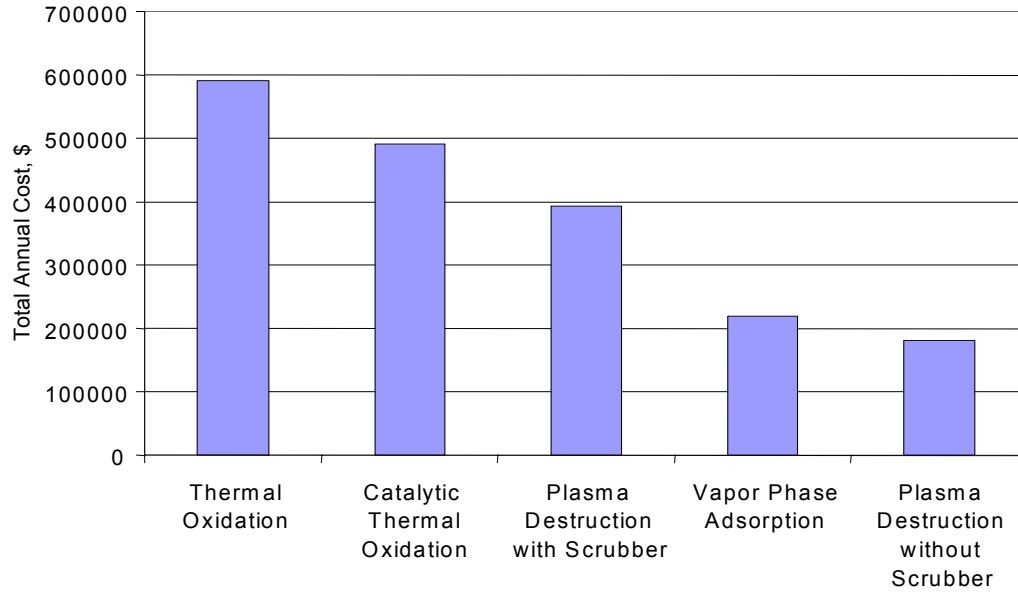


Figure 4: Total Annual Cost Comparison of Compounds at 20,000 cfm and 2000 ppm

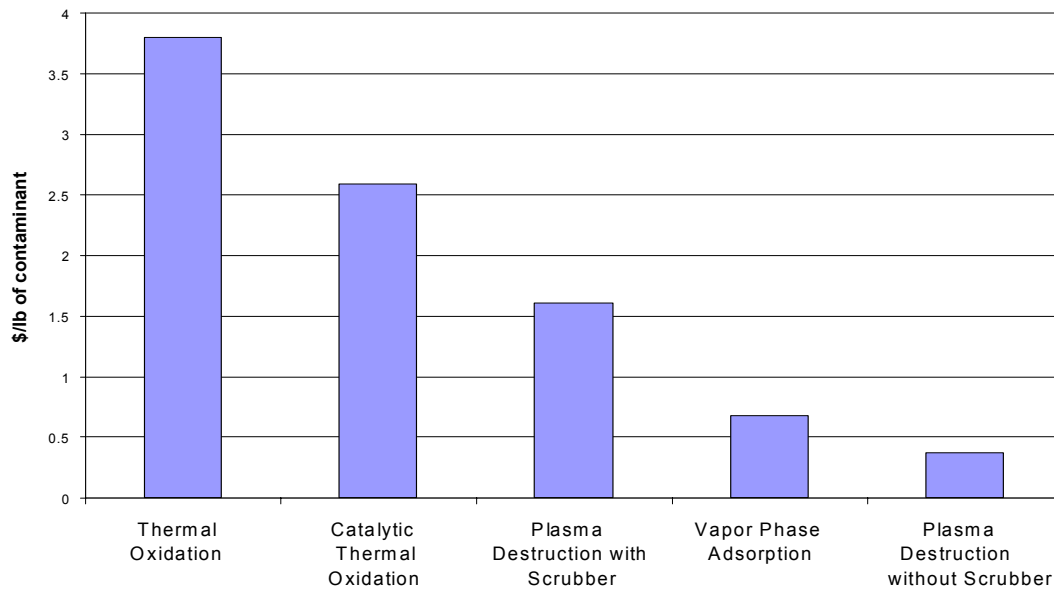


Figure 5: Removal Cost per Unit Contaminant at 20,000 cfm and 2000 ppm

2.5. Corona Chemistry of Toluene

Numerous reactions may take place in a DBD plasma reactor that can lead to the formation of active species capable of reacting with pollutant molecules. These species react with pollutant molecules, which can result in near complete oxidation of hydrocarbons into CO, CO₂, H₂O and conversion of species such as Cl, S and NO into HCl, Cl₂, SO₂, H₂SO₄, HNO₃ (Coogan, 1997).

If the concentration of the active species is high enough to initiate the destruction reaction, the pollutant concentration decreases. The complete reaction chemistry is extremely complicated. The reactant molecules are known to undergo a series of intricate intermediate reactions before breaking down completely destroying into combustion products (Agnihotri, 2003).

Due to the complexities of these mechanisms for pollutant destruction in DBD plasma reactors, additional research needs to be done in the mechanism of the reaction.

However, it is not necessary to understand the mechanism of plasma destruction of pollutants completely to gain valuable information about the pollutant destruction process. Recent research has shown that simplified kinetic models can be used to describe the rate of radical-initiated decomposition of the pollutant molecules in the reactor (Agnihotri, 2003).

Toluene:

The destruction of toluene in a plasma reactor occurs through oxidation. A possible free radical mechanism for the oxidation of toluene in the reactor is discussed below.

Toluene can either react with the atmospheric oxygen or the hydroxyl radical once a mixture of radicals is formed in the reactor. The following reactions show one possible mechanism of toluene destruction in the DBD plasma reactor (Nunez, 1993)



or



The formation of the benzyl radical leads to the following series of reactions:





2.6. Destruction Studies of Toluene

Several studies have been performed by various researchers on the destruction of different chemicals when exposed to plasma. Nunez (1993) used packed bed reactor for the destruction of toluene. Agnihotri studied the relationship between the energy density and destruction efficiency for toluene using planer DBD reactor. The relationship between DRE and power density can be expressed as (Agnihotri, 2003)

$$\frac{[X]}{[X_0]} = \exp\left[-\frac{P}{Q\beta}\right] \quad (11)$$

where $[X]$ and $[X_0]$ are pollutant concentrations in the outlet and inlet streams in ppmv, respectively; P is the average power delivered to the plasma cell in watts; Q is the flow rate of gas in liters/second; β is the scaling parameter for pollutant X in joules/liter; By plotting P/Q (y axis) vs. $-\ln [X]/ [X_0]$ (x axis) gives a straight line passing through the origin with a slope value of β (Agnihotri, 2003).

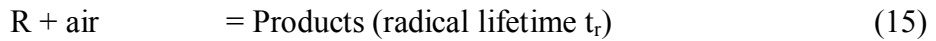
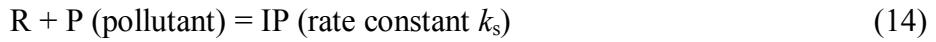
Agnihotri (2003) also gave β parameters for some common pollutants calculated for a planer DBD plasma reactor are shown in the Table 1.

Table 1: Scale up Parameter, β for Various Compounds.

| Compound | β (Joules/liter) |
|--|------------------------|
| Perchloroethylene, PCE | 1500 |
| NO _x | 66 |
| Trichloroethylene, TCE | 33 |
| Carbon Tetrachloride, CCl ₄ | 2500 |
| Toluene | 99 (Yan, 2001) |

$$\beta = (1/Gt_r k_s) + [X_O]/G \quad (12)$$

G is the production efficiency of the radical species responsible for pollutant destruction; k_s is the radical-pollutant kinetic rate constant, and t_r is the lifetime of the pollutant attacking species (Rudolph, 2001). The general destruction process is visualized as radical production, radical-pollutant interaction, and radical scavenging by air molecules.



One of the goals of this study was to calculate the scale up parameter using single tube single DBD reactor and to determine if the parameter is independent of the reactor configuration. In addition this study was conducted to evaluate the effect of secondary voltage, frequency and flow rate on the destruction efficiency (DRE). Knowledge of an approximate value of β can be used to determine the power requirements for a given DRE and flow rate of gas stream (and hence the name scale up parameter).

3. Methods and Materials

This chapter gives the detailed experimental procedures, data analysis and the design used in this research project. This chapter is divided into two main parts to discuss the components mentioned above.

1. Experimental Setup, and
2. Experimental Design

3.1. Experimental Setup

Experimental set up is divided into four different components. They are

1. Reactor system,
2. Plumbing system,
3. Electrical system, and
4. Analysis system.

3.1.1. Reactor System

Single Tube Single Dielectric Reactor

The single tube single dielectric reactor used in this work was made of quartz (Technical Glass Products Inc.) glass tube (dielectric constant of 3.8 and dielectric strength of 25-40 kV/mm) with a 10 mm inner diameter and a 1 mm wall thickness with copper tape (Mc Gills Warehouse) as the outer electrode (Veenstra, 2003). The length of the outer electrode is 10 cm. The inner high voltage electrode consisted of a stainless steel rod (Stillwater Steel Supply, Stillwater) 1.59 mm in diameter. The total volume of the reactor is 1963 mm³ (1.963 ml). Hydraulic radius of the reactor is 1.25 mm (Diameter/4). Figure 6 shows the dimensions of the reactor. A photograph of the reactor is shown in Figure 7.

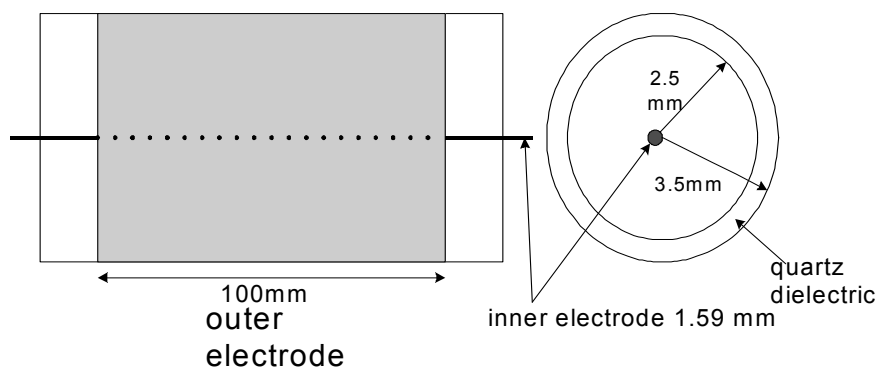


Figure 6: Dimensions of Single Tube Single Dielectric Reactor

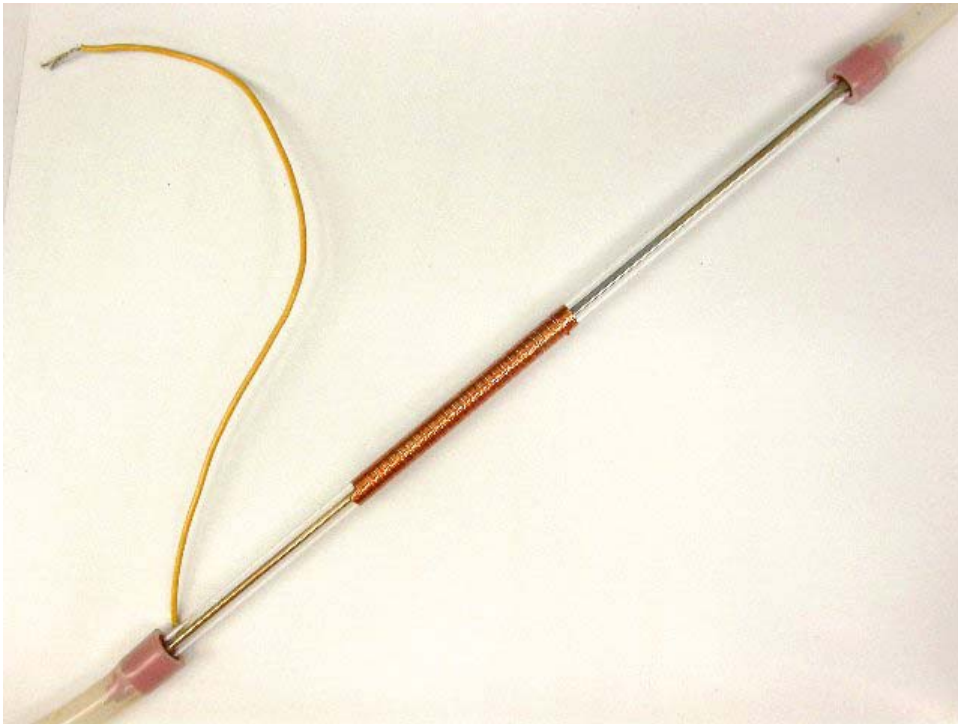


Figure 7: Single Tube Single Dielectric Reactor

3.1.2. Electrical system

The driving force for the plasma reactor is electricity. The schematic of electrical set up is shown in Figure 8.

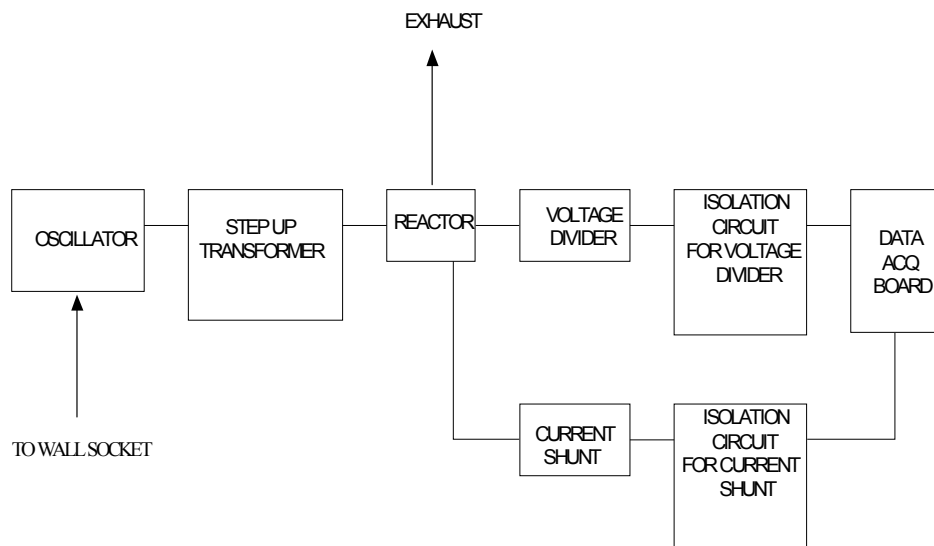


Figure 8: Electrical System of Plasma Unit

The three basic systems in this electrical set up are the oscillator, the transformer, and the secondary voltage and current measuring circuit.

The power from the wall socket is applied through a California Instruments Model 161 T oscillator. The oscillator range is from 40-5000 Hz, with a primary maximum of 120 V_{rms}. Figure 9 shows a photograph of the oscillator.



Figure 9: Oscillator

This output voltage was stepped up to 15kV using a Franceformer model 15060P, 890VA center-tapped, luminous-tube transformer (Jefferson Electric). The electrodes of the plasma reactor were connected to the high-voltage; secondary terminals of this transformer by 8 mm multi thread silicone coated wires (Taylor Pro wire, Radio Shack Inc). When energized, this circuit created a plasma discharge within the reactor. The transformer is shown in Figure 10.



Figure 10: Transformer

The maximum voltage drop across the reactor was 15kV_{rms} . This voltage was too large to measure directly so a custom designed voltage divider was used to step the voltage down to a measurable value. Figure 11 shows the circuit used to measure the voltage across the reactor. Figure 12 shows the secondary power source for circuits used to measure the secondary voltage and secondary current.

Voltage across the reactor and current through the reactor were monitored using a computerized data acquisition system. Each measured variable produces an electrical signal as output. Using Lab View software (National Instruments) these signals can be read and plotted. To monitor these signals, a data acquisition (DAQ) board was used. DAQ boards read both analog and digital signals (Figure 13). The DAQ board must be protected from the high voltages used to energize the plasma reactors because it can only withstand inputs in the range of $\pm 15\text{V}$. Isolation amplifiers were used to protect the DAQ board.

An isolation amplifier acts as an interface between external devices and the data acquisition system (Veenstra, 2003). It provides galvanic isolation between the input and output. The outputs from all of the isolation amplifiers were connected to each channel of the DAQ board. Lab View software was used to program the DAQ board.

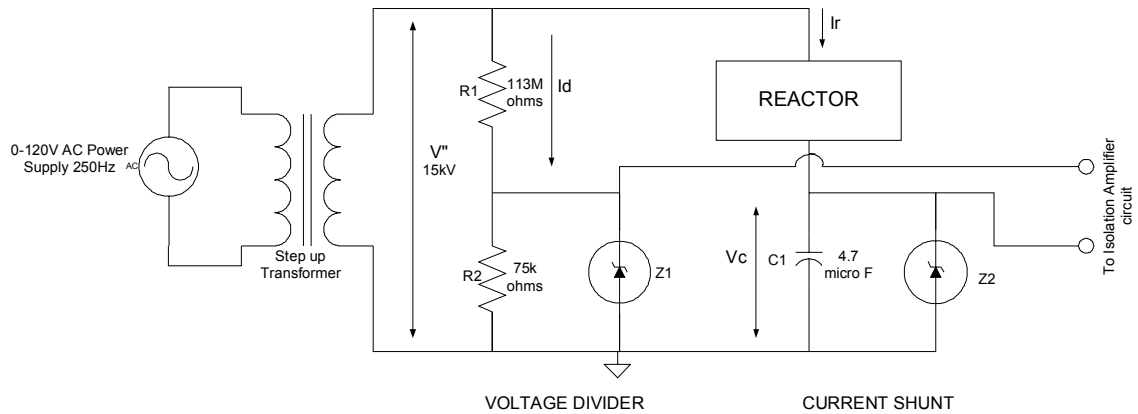


Figure 11: Voltage and Current Measuring Circuit



Figure 12: Secondary Power Source

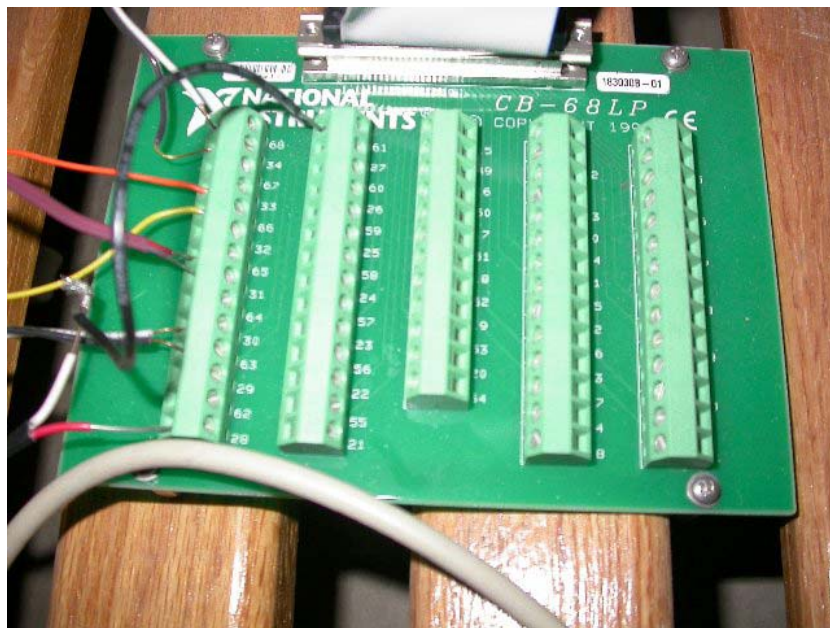


Figure 13: Data Acquisition Board

3.1.3. Plumbing System

A schematic of the plumbing system is shown in Figure 14. This section explains how all the parts are connected to each other. This also gives the materials used to connect all the equipments. The following equipment was used in this research:

- Mass flow controller (Brooks 5800 TR),
- Mass flow meter (LINDE FM 4575),
- Syringe pump (Harvard Apparatus Model '22'), and
- SRI 8610C gas chromatograph with flame ionization detector.

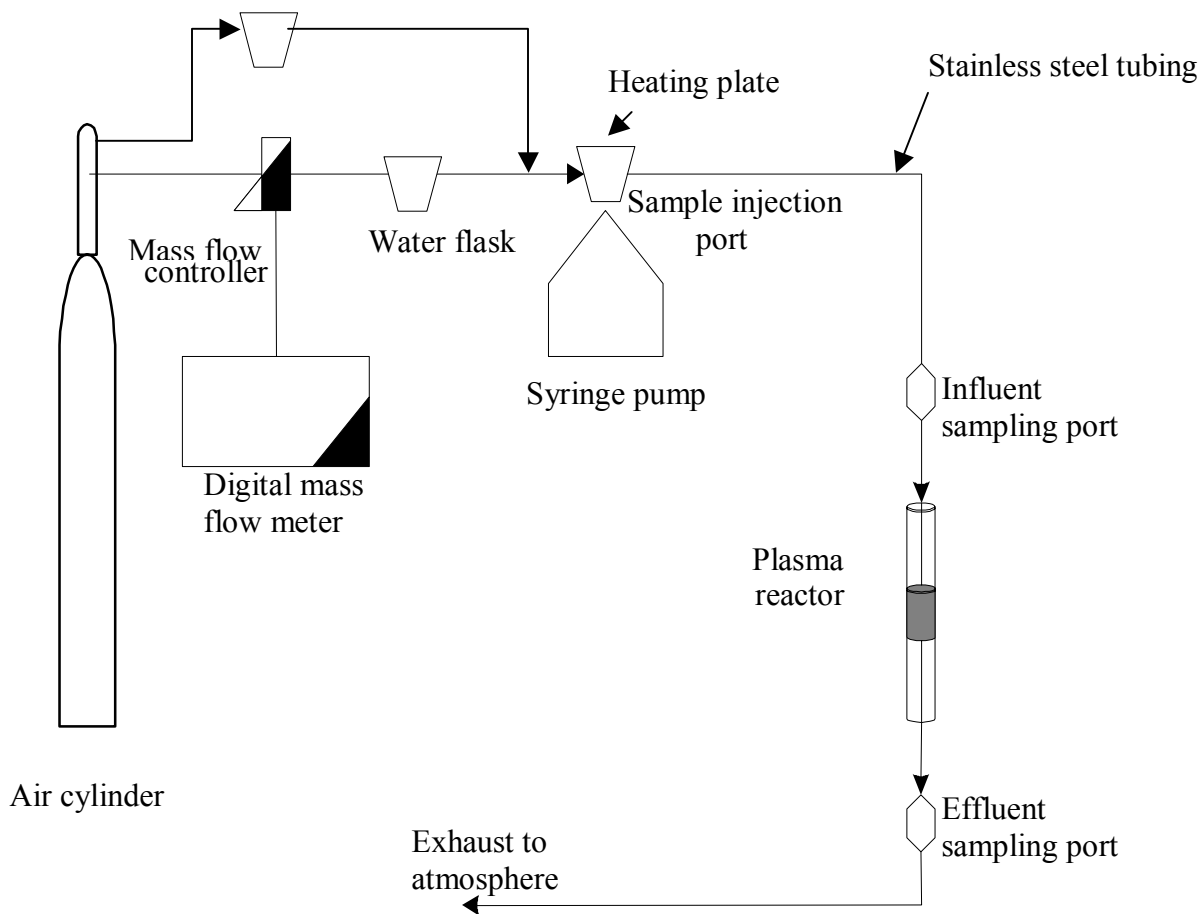


Figure 14: Plumbing System

The zero grade air supplied from a compressed gas cylinder was regulated through the Brooks mass flow controller (Figure 15) and the rotameter. The mass flow control panel (Brooks 5800 TR) diagram is shown in Figure 16. The mass flow controller has two different modules, which can provide a range of flow rates. In this research one mass flow module (channel 3) was used which could provide up to 800 ml/min of gas flow and the rotameter with a maximum capacity of more than 10,000 ml/min.



Figure 15: Mass Flow Controller



Figure 16: Mass Flow Controller Panel

The compressed air line was divided into two different lines. One of these lines was used to control the humidity of the air by passing it through a water saturator, which consisted of one 500 ml Erlenmeyer flask half filled with tap water. The second line was passed through the rotameter and joined with the first line after it exited the water saturator. This line leads to the sample injection port where the contaminants were injected into the air flow line using Harvard Apparatus Model '22' syringe pump (Figure 17). Liquid toluene was injected into the airflow line through a rubber septum in a 2.5 ml glass injection port.

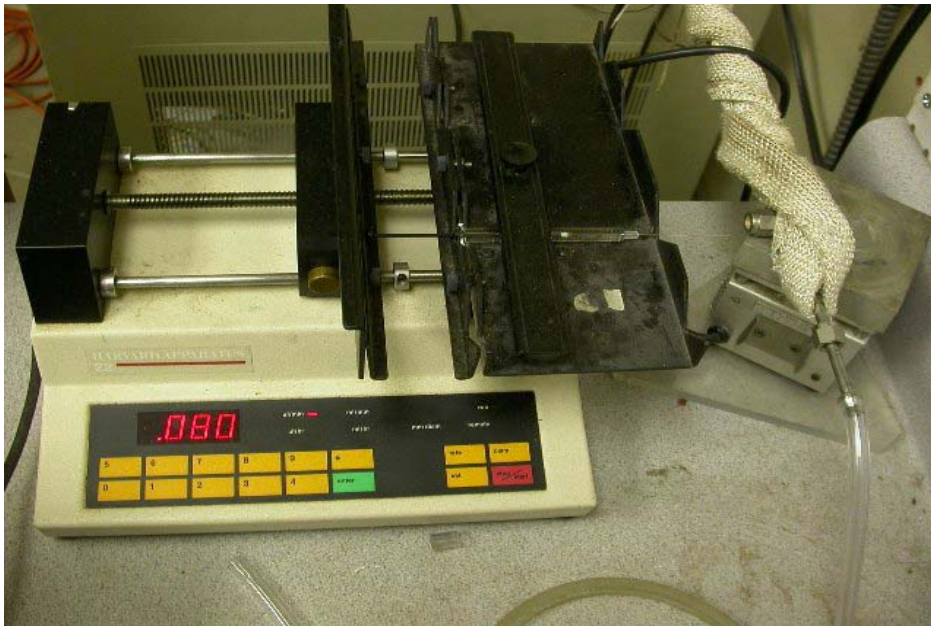


Figure 17: Syringe Pump

The syringe pump was fitted with a 100 μ l Hamilton Gastight series syringe (Supelco Inc.). Injection rate was set to achieve a total concentration of 100 ppm of toluene in the air stream. The calculations for the required injection rates are shown in Appendix C.

The injection port was maintained at a temperature of 65°C using an Omega DP 465 thermostat (Figure 18) heating plate to vaporize all the components in the mixture.



Figure 18: Thermostat

The influent sample was taken from the inlet sampling port 20 cm before the reactor. The gas coming out of the plasma reactor exits from the outlet sampling port (20 cm approximately after the reactor) to the atmosphere. This outlet sampling port is the location where the effluent samples are taken. These inlet and outlet sampling bombs had a rubber septum through which the 0.5 ml of samples was taken in a Hamilton 1002SL 2.5 ml gas tight syringe fitted with a sample lock. The samples were analyzed in SRI 8610C Gas Chromatograph (GC). The GC photograph is shown in Figure 19.



Figure 19: Gas Chromatograph Unit

Humidity was monitored using a Davis instrument model DTH-1 Digital Hygrometer/Thermometer at the exit of the reactor. The entire piping system is made of welded stainless steel and teflon tubing which is used due to its non reactivity with chemicals. The stainless steel has an inner diameter of 0.635 cm and a thickness of 0.0889 cm. The teflon had an inner diameter of 0.635 cm and a thickness of 0.159 cm.

3.1.4. Analysis system

Destruction tests were performed with varying voltage, frequency, residence time, and energy density, while keeping all the other parameters constant. The objective was to study the effect of each parameter on the destruction of the VOCs.

Before beginning the destruction tests, the following calibrations were completed:

- Linde mass flow modules were calibrated for flow rate of air up to 745 ml/min using the digital mass flow meter and the calibration data are attached in Appendix D.
- Rotameter was calibrated for flow rates up to 12,812 ml/min and these data are included in the Appendix E.
- SRI 8610C Gas Chromatograph (GC) was calibrated for toluene, CO and CO₂.

This calibration procedure will be discussed in the results section.

Calibration Procedure for the Plasma Reactor

The procedure to calibrate toluene in the GC was as follows:

- 1) The peak sample method was first selected on the computer.
- 2) The Flame Ionization Detector (FID) was switched ON after turning ON the gas flows. The gas flows used were:
 - a. Hydrogen - 25 ml/min
 - b. Air – 250 ml/min
 - c. Helium – 10 ml/min
- 3) The FID was set at a temperature of 150°C.
- 4) The oven temperature was set at 70°C.

- 5) A known volume of custom made standard (Scotty Gases) which had 102 ppm toluene was injected into a GC.
- 6) 0.01, 0.02, 0.03, 0.04, 0.05, 0.1, 0.2 ml volumes were used for the calibration.
- 7) After injecting the sample, the run was initiated by pressing the 'space bar' key on the computer.
- 8) The GC operating program integrates the peak area for each component and stores the data.
- 9) The runs were performed three times for each sample volume or until a +5% or -5% repeatable area was obtained. The average area was taken for the calibration plot.
- 10) A calibration plot was obtained by plotting the component mass (Y-axis) versus average area (X-axis).
- 11) Once the GC is calibrated, the unknown samples can be injected according to the above procedure and the calibration plot that was obtained is used to find the concentration.

Calibration Procedure for the Carbon Balance

The procedure to calibrate CO and CO₂ in the GC was as follows:

- 1) The peak sample method was first selected on the computer.
- 2) The detector (FID) was switched ON after turning ON the gas flows. The gas flows used were:
 - a. Hydrogen - 25 ml/min
 - b. Air – 250 ml/min
 - c. Helium – 10 ml/min

- 3) The FID was set at a temperature of 380°C.
- 4) The Oven temperature was set at 70°C.
- 5) A known volume of custom made standards (Scotty Gases), which had CO, and CO₂ of 500 and 476 ppm, respectively was injected into a GC.
- 6) 0.1, 0.2, 0.3, 0.4, 0.5, 0.6, 0.7, 0.8, 0.9, 1.0 ml volumes were used for the calibration.
- 7) After injecting the sample, the run was initiated by pressing the ‘space bar’ key on the computer.
- 8) The GC operating program integrates the peak area for each component and stores the data.
- 9) The runs were performed three times for each sample or until a +5 or –5 % of repeatable area was obtained. The average area was taken for the calibration plot.
- 10) A calibration plot was obtained by plotting the component mass (Y-axis) versus average area (X-axis).
- 11) Once the GC is calibrated, the unknown samples can be injected according to the above procedure and the calibration plot that was obtained is used to find the concentration.

General Operating Procedure for the GC:

The reactants and the products from the plasma reactor were analyzed using the SRI Model 8610C Gas Chromatograph (GC) with a Flame Ionization Detector (FID). A dimethyl polysiloxane MXT-1 capillary column (manufactured by Restek) was used in this work. The capillary column was 15 m long with an inner diameter of 0.53 mm and a film thickness of 5 microns. The operating procedure is as follows.

- 1) The detector (FID) was switched ON after turning ON the gas flows. The gas flows used were:
 - a. Hydrogen - 25 ml/min (for FID)
 - b. Air – 250 ml/min (for FID)
 - c. Helium – 10 ml/min (carrier gas)
- 2) The FID was set at a temperature of 380°C.
- 3) The oven temperature was set at 70°C.
- 4) Influent and effluent samples collected at 1, 5, 10, 20, 25, 30 and 35 minutes were analyzed.

General Operating Procedure for the Experiment:

1. Zero grade air from a cylinder was passed through the reactor.
2. The injection rate was set to achieve a total concentration of 100 ppm of toluene in the air using the syringe pump.
3. The desired humidity is achieved by varying the flow rate of air through the water saturator from the mass flow controller (usually 40% through the mass flow controller and water saturator and the remaining through the rotameter).
4. Gas stream into the reactor is allowed to reach steady state. This is checked by the influent and effluent concentration.
5. After the desired stabilization is achieved an influent sample was taken and analyzed in the GC before start the experiment. The volume of sample collected was 0.5ml, collected in a Hamilton 1002SL 2.5 ml gas tight syringe fitted with a sample lock.
6. Effluent samples were collected from the exit of the reactor at 1, 5, 10, 15, and 20 minutes after the power source was switched on, and injected into SRI

8610C Gas Chromatograph (GC) for analysis.

7. The reactor was switched off at 20 min. Effluent samples were collected from the exit at 25 and 30 minutes and analyzed in the GC.
8. Finally the influent sample was taken at 35 min to complete the single run and analyzed in the GC.

3.2. Experimental Design

This section explains the procedure used to determine the effect of varying secondary voltage, frequency, flow rate, and energy density on the destruction efficiency.

3.2.1. Secondary Voltage Variation

Three different values were selected to show the effect of secondary voltage on the energy density and the destruction on the toluene. The selected values are 9000V, 12,000V and 15,000V. These were selected due to the operating limitations of the equipment and the optimum range of values (Veenstra, 2003). All three runs were tested at constant 100 ppm toluene inlet concentration, 300 Hz frequency, 30-45 % relative humidity and a flow rate of 10 ml/s. Since secondary voltage can be controlled only through the primary voltage, it is not possible to maintain a constant secondary voltage. The actual secondary voltage varied between +5 or -5 % of the ideal value. Inlet concentration of toluene also varies between +20 or -20 % of the ideal value. It is critical to have constant inlet concentration of 100 ppm. But once the concentration reached equilibrium, it maintained constant value. The actual secondary voltage, secondary current and power factor were measured for each run. Energy density values were calculated from these measured values (power/flow rate). The matrixes of all the runs are tabulated in the Table 2. This table shows the theoretical list of experiments. From all the runs conducted, the effect of secondary voltage on the energy density was analyzed.

Table 2: Matrix of Runs for Single Tube Single Dielectric Plasma Reactor with 10 cm Outer Electrode Length

| Variable and Run No | Flow rate (mL/s) | Frequency (Hz) | Theoretical Secondary Voltage (V) | Actual Secondary Voltage (V) | Secondary Current (A) | Power Factor (pf) | Energy Density (J/L) |
|---------------------|------------------|----------------|-----------------------------------|------------------------------|-----------------------|-------------------|----------------------|
| Secondary voltage | | | | | | | |
| 1 | 10.0 | 300 | 15000 | | | | |
| 2 | 10.0 | 300 | 12000 | | | | |
| 3 | 10.0 | 300 | 9000 | | | | |
| Frequency | | | | | | | |
| 4 | 10.0 | 300 | 15000 | | | | |
| 5 | 10.0 | 250 | 15000 | | | | |
| 6 | 10.0 | 200 | 15000 | | | | |
| Flow rate | | | | | | | |
| 7 | 10.0 | 300 | 15000 | | | | |
| 8 | 8.0 | 300 | 15000 | | | | |
| 9 | 6.0 | 300 | 15000 | | | | |
| Energy Density | | | | | | | |
| 10 | 10.0 | 250 | 11250 | | | | |
| 11 | 10.0 | 250 | 15000 | | | | |
| 12 | 8.0 | 200 | 11250 | | | | |
| 13 | 8.0 | 300 | 15000 | | | | |
| 14 | 6.0 | 300 | 15000 | | | | |
| 15 | 6.0 | 300 | 12000 | | | | |
| 16 | 6.0 | 300 | 9000 | | | | |

Bold letters indicates where duplicate runs were conducted.

Blank space indicates the values to be measured or calculated.

(Inlet concentration=100 ppm and Relative Humidity=30-45% for all the runs)

3.2.2. Frequency Variation

The effect of frequency on the destruction of toluene was tested through three different frequencies, 200 Hz, 250 Hz, and 300 Hz. These were selected due to the operating limitations of the equipment and the optimum range of values (Veenstra, 2003). All three runs were conducted at 100 ppm of toluene, 10 ml/s flow rate, 30-45% of relative humidity, and 15,000V ideal secondary voltage. The actual secondary voltage varied between +5 or -5 % of the ideal value. The actual secondary voltage, secondary current and power factor were measured for each run (Table 2). Energy density values were calculated from these measured values (power/flow rate). Inlet concentration of toluene also varies between +20 or -20 % of the ideal value. Data from all the runs, would allow a reasonable effect of frequency on the energy density and the destruction of toluene to be evaluated.

3.2.3. Flow Rate Variation

To measure the effect of flow rate, three different flow rates 6, 8, and 10 ml/s (0.33, 0.24, and 0.20 sec residence time, respectively) were tested in the reactor. These were selected due to the operating limitations of the equipment and the optimum range of values (Veenstra, 2003). All three runs were conducted at 100 ppm of toluene, 300 Hz frequency, 30-45% relative humidity, and 15,000V ideal secondary voltage. The actual secondary voltage varied between +5 or -5 % of the ideal value. The actual secondary voltage, secondary current and power factor were measured for each run (Table 2). Energy density values were calculated from these measured values (power/flow rate). Inlet concentration of toluene also varies between +20 or -20 % of the ideal value. Data

from all the runs, would allow a reasonable effect of flow rate on the energy density and the destruction of toluene to be evaluated.

3.2.4. Energy Density Variation

The effect of energy density on the destruction of toluene was assessed by using seven different energy density values. The seven different runs lead to seven different energy densities by changing flow rate, frequency or secondary voltage. All the runs were run at constant 100 ppm toluene with a humidity ranging from 30 to 45 %RH. Flow rates (6, 8, 10 ml/s), frequencies (200, 250, 300) and secondary voltages (9000, 12,000, 15,000) were varied to achieve the different energy densities. The actual secondary voltage varied between +5 or -5 % of the ideal value. The actual secondary voltage, secondary current and power factor were measured for each run (Table 2). Energy density values were calculated from these measured values (power/flow rate). Inlet concentration of toluene also varies between +20 or -20 % of the ideal value. This will allow a reasonable observation of the effect of energy density on the destruction efficiency of toluene.

3.2.5. Detection of Byproducts

The major by-products expected during the runs are CO and CO₂ (Korzekwa, 1998). The byproducts produced during each destruction run were obtained whenever the sample (toluene) was analyzed in the GC.

3.2.6. Carbon Balance

The overall carbon mass balance was calculated for the products entering and exiting the plasma reactor during the destruction runs of 100 ppm of toluene

concentration. This procedure was estimated by subtracting the total carbon byproducts coming out of the reactor from the total carbon entering.

$$\text{Residual Carbon} = \text{Mass of carbon in the inlet stream} - \text{Mass of carbon in the outlet stream} \quad (16)$$

The carbon products coming out of the reactor were measured by the methanizer (SRI Instruments), which is located before the FID and after the column in the GC unit.

The schematic of the methanizer with FID is shown in the Figure 20.

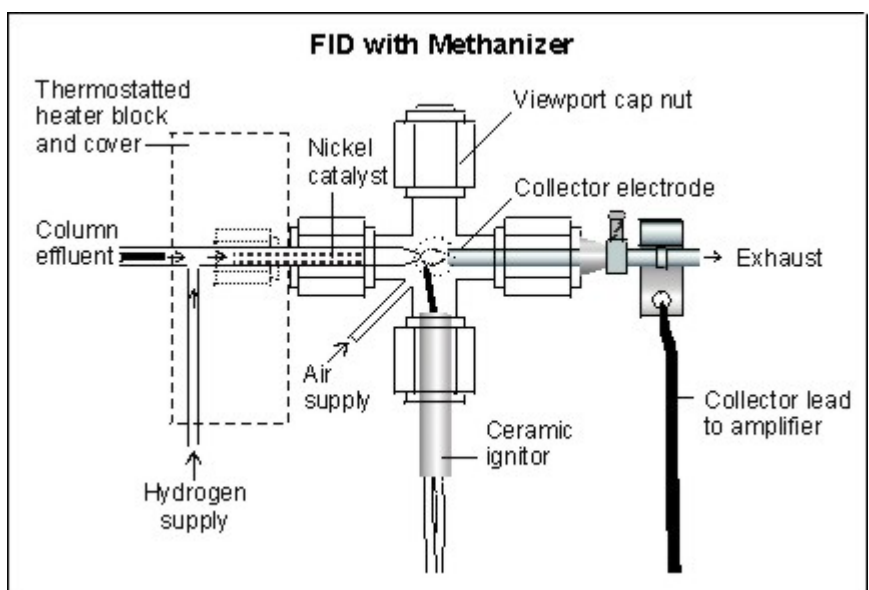


Figure 20: Methanizer (SRI Instruments)

When the column effluent mixes with the FID hydrogen supply, the methanizer converts all the carbon monoxide and carbon dioxide compounds into methane by using a nickel catalyst at 380° C and gives the respective peak which indicates the concentration of carbon monoxide and carbon dioxide. The methanizer leaves the hydrocarbons unaffected.

4. Results and Discussion

4.1. Calibration Data for the Plasma Reactor

To measure the concentration of toluene, CO and CO₂ during destruction, standardization of these compounds in the GC is necessary. The results obtained during standardization are as follows.

1. The injection volume of toluene and its mass is calculated using the ideal gas law and the calculation is attached in the Appendix F.
2. Various injection volumes and their respective areas during calibration are tabulated in Appendix G.
3. A graph is plotted using influent mass against the average area obtained. Figures 21, 22 and 23 shows representative calibration curves for toluene, CO and CO₂, respectively.
4. The minimum detection limit of toluene was found to be 1.8 ppm (4.3E-09 g).

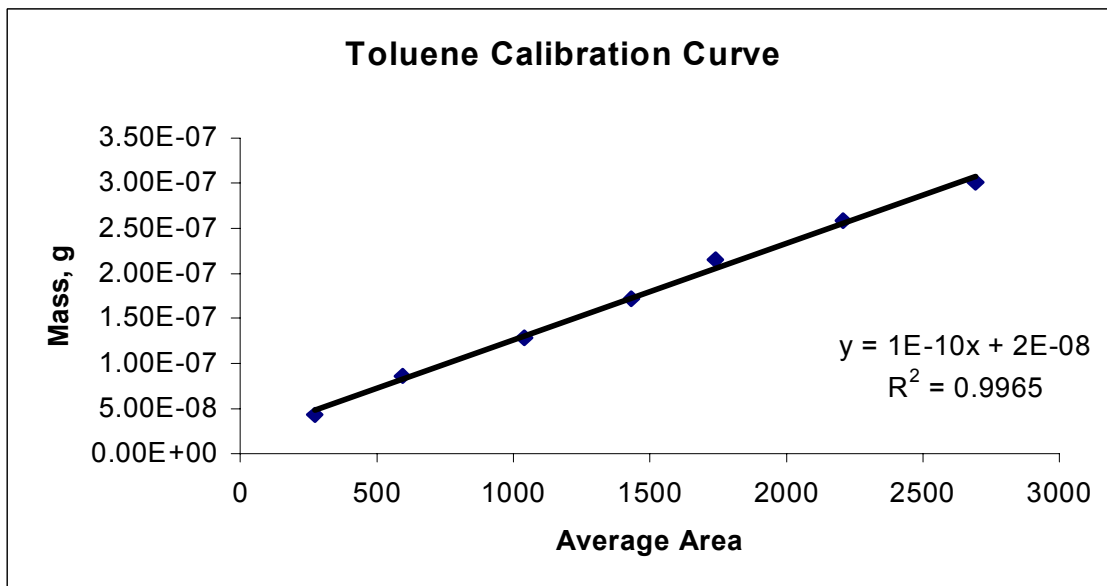


Figure 21: Toluene Calibration Curve

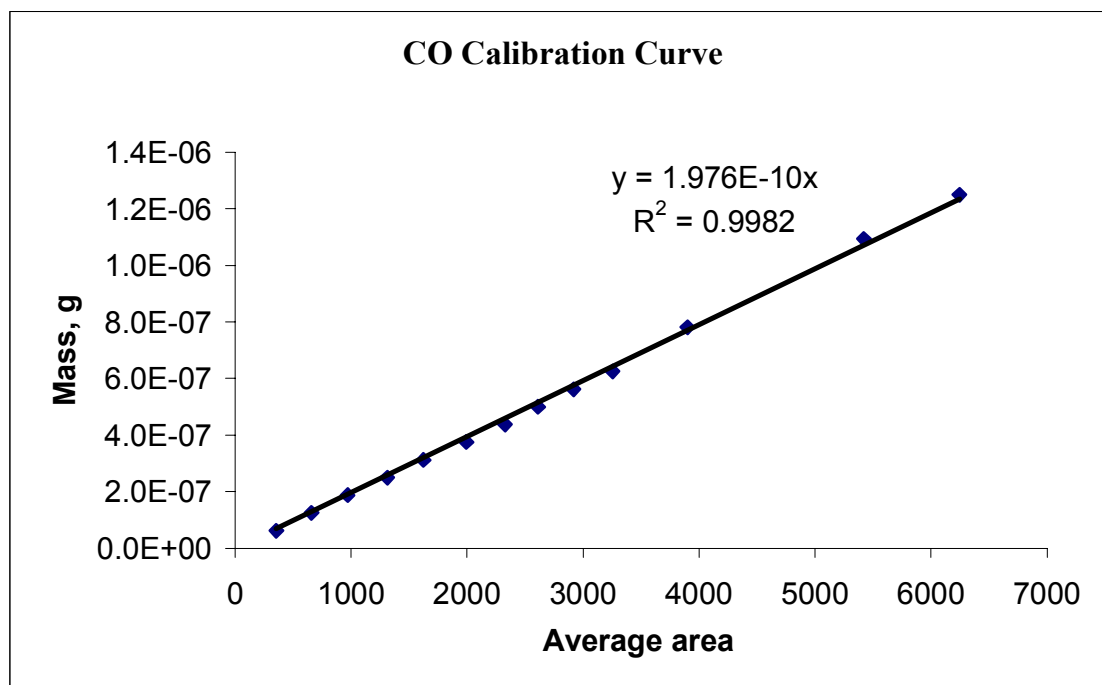


Figure 22: CO Calibration Curve

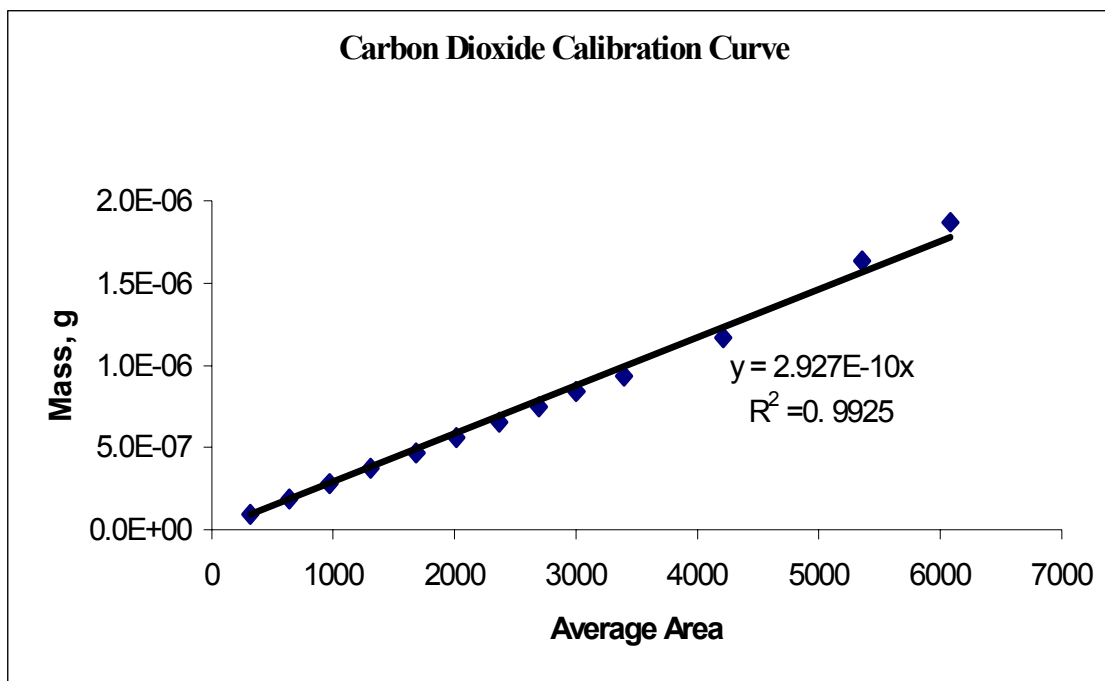


Figure 23: Carbon Dioxide Calibration Curve

4.3. Effect of Secondary Voltage on Destruction

The selected test values at 9000V, 12,000V and 15,000V gave destruction efficiencies of 96.6, 90.0, and 96.8%, respectively at a constant 100 ppm toluene concentration, flow rate of 10 ml/s, 30-45% relative humidity and frequency 300 Hz (See Table 2 for matrix of runs). From all of the runs conducted the results shows that increasing the secondary voltage increased the destruction of toluene only when there was an increase in energy density. Figures 24, 25, and 26 shows destruction data for three different secondary voltages. Table 3 shows the effect of secondary voltage on the destruction of toluene. Actual operating values for the runs and energy density calculation are shown in Appendix H.

$$\text{Energy density} = (\text{Secondary voltage} * \text{Secondary Current} * \text{Power factor}) / \text{Flow rate} \quad (17)$$

Agnihotri (2003) reported that an increase in secondary voltage increased the destruction efficiency. Korzekwa (1998) also showed that an increase in energy density above 95% DRE, negligible increased destruction efficiency. In this case changing the secondary voltage changes the energy density and the higher the energy density, the higher the destruction.

Table 3: Effect of Secondary Voltage on Destruction of Toluene

| Actual Secondary Voltage (V) | Secondary Current (A) | Power Factor | Energy Density (J/l) | Influent Concentration (ppm) | Effluent Concentration at 20 min (ppm) | Destruction Efficiency (%) |
|------------------------------|-----------------------|--------------|----------------------|------------------------------|--|----------------------------|
| 15,509 | 0.005 | 0.571 | 4428 | 97.1 | 3.1 | 96.8 |
| 12,332 | 0.003 | 0.726 | 2686 | 116.6 | 11.7 | 90.0 |
| 9,251 | 0.006 | 0.705 | 3904 | 79.4 | 2.7 | 96.6 |

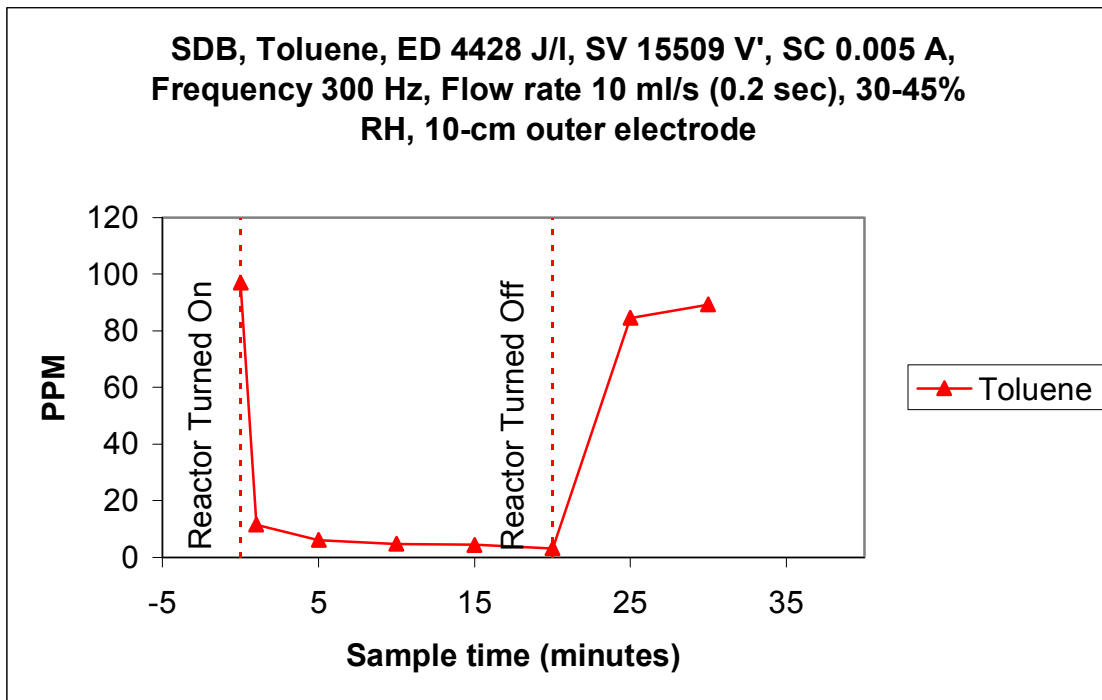


Figure 24: Destruction Run at 15000 Secondary Voltage

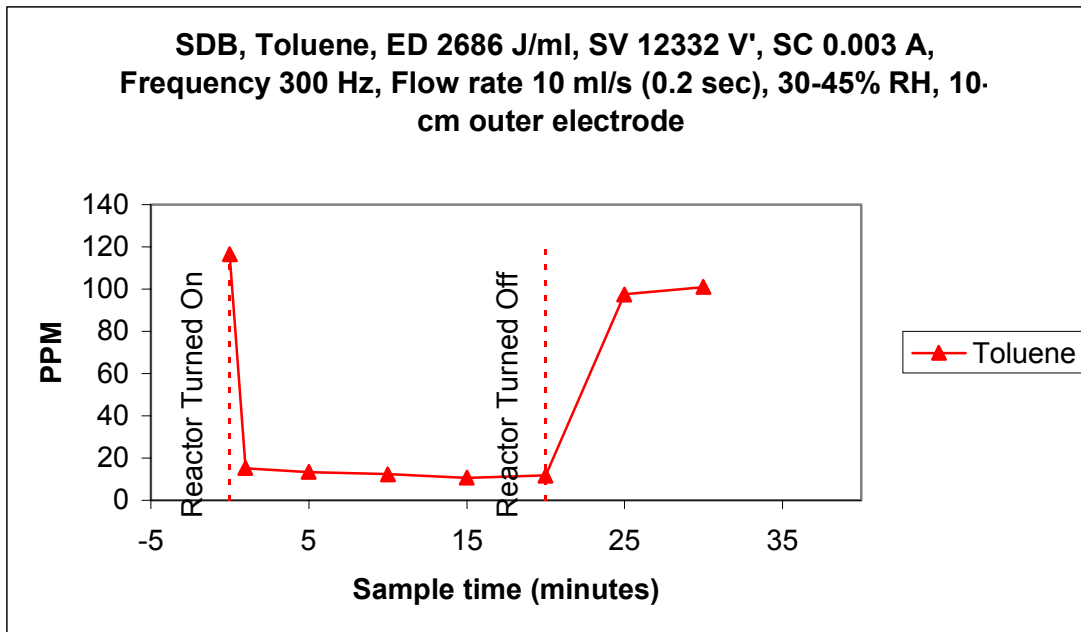


Figure 25: Destruction Run at 12000 Secondary Voltage

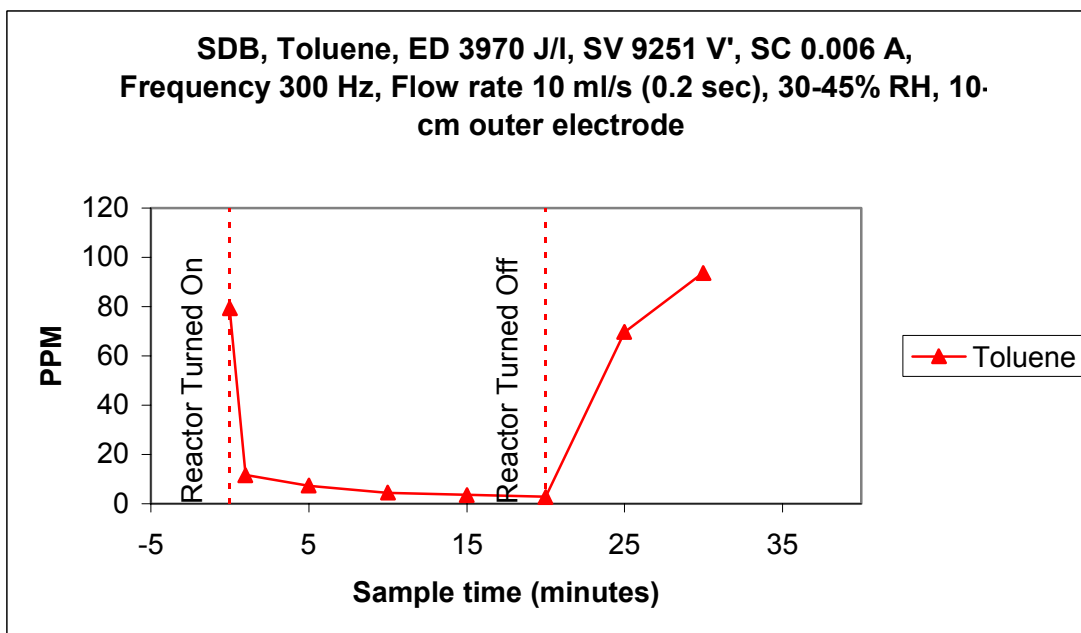


Figure 26: Destruction Run at 9000 Secondary Voltage

4.4. Effect of Frequency on Destruction

Three different frequencies were tested in the reactor: 200 Hz, 250 Hz, and 300 Hz. All three tests were performed at a constant 100 ppm toluene concentration, flow rate of 10 ml/s and 30-45 % relative humidity with a secondary voltage of 15,000 (approximately). The actual secondary voltages for the frequency 200, 250, 300 were 15,203, 15,649, and 15,509 respectively. Destruction efficiency increased with increasing frequency (energy density also increased). Table 4 shows the effect of frequency on the destruction of toluene at a constant energy density. Figures 27, 28, and 29 shows the destruction efficiencies at 200, 250 and 300 Hz respectively.

Ahmad (1996) showed that an increase in frequency give better destruction of toluene at a constant inlet concentration, primary voltage and flow rate, but energy density also increased indirectly.

Table 4: Effect of Frequency on Destruction of Toluene

| Frequency (Hz) | Secondary Current (A) | Power Factor | Energy Density (J/l) | Influent Concentration (ppm) | Effluent Concentration at 20 min (ppm) | Destruction Efficiency (%) |
|-----------------------|------------------------------|---------------------|-----------------------------|-------------------------------------|---|-----------------------------------|
| 300 | 0.005 | 0.571 | 4428 | 97.1 | 3.1 | 96.8 |
| 250 | 0.003 | 0.710 | 3333 | 104.2 | 4.0 | 96.1 |
| 200 | 0.002 | 0.650 | 2570 | 119.6 | 16.8 | 86.0 |

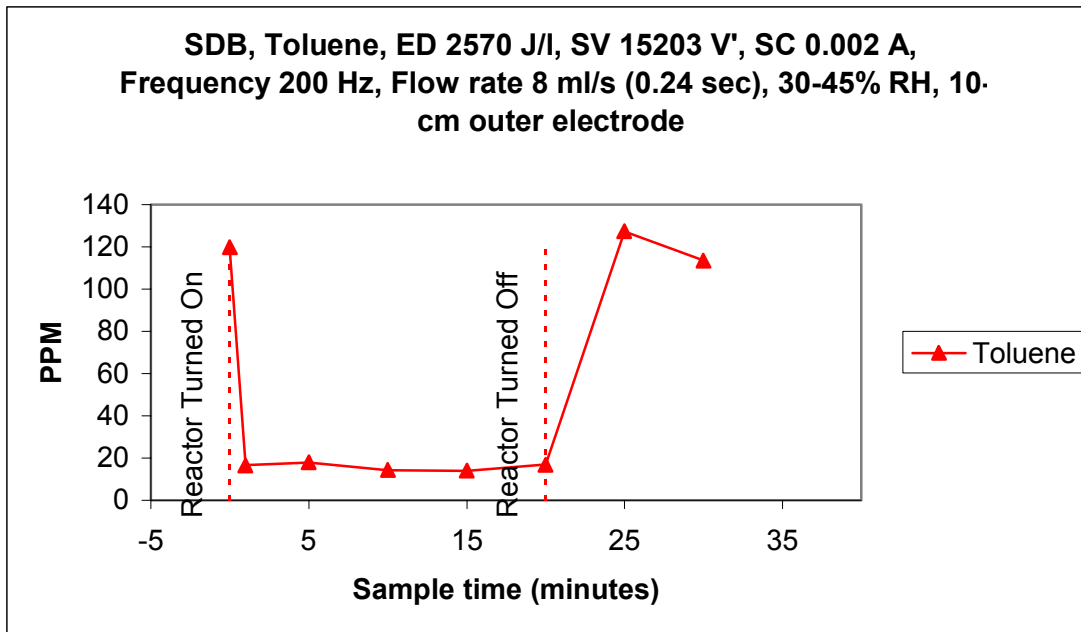


Figure 27: Destruction Run at 200 Hz Frequency

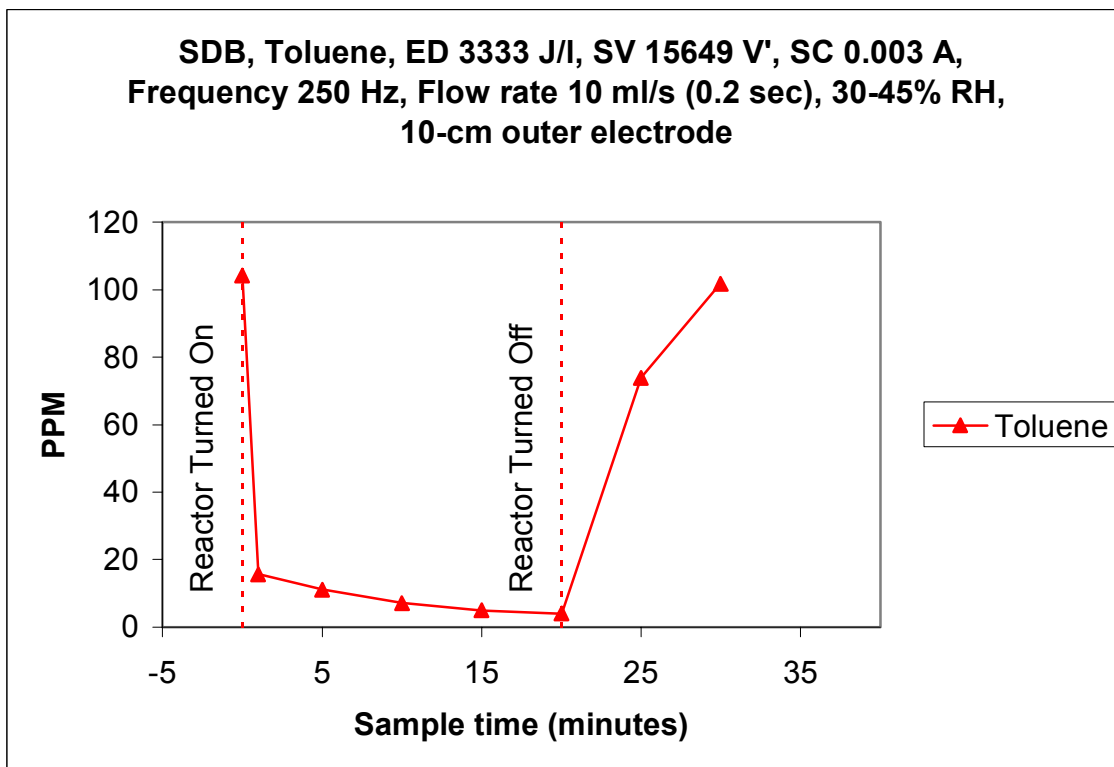


Figure 28: Destruction Run at 250 Hz Frequency

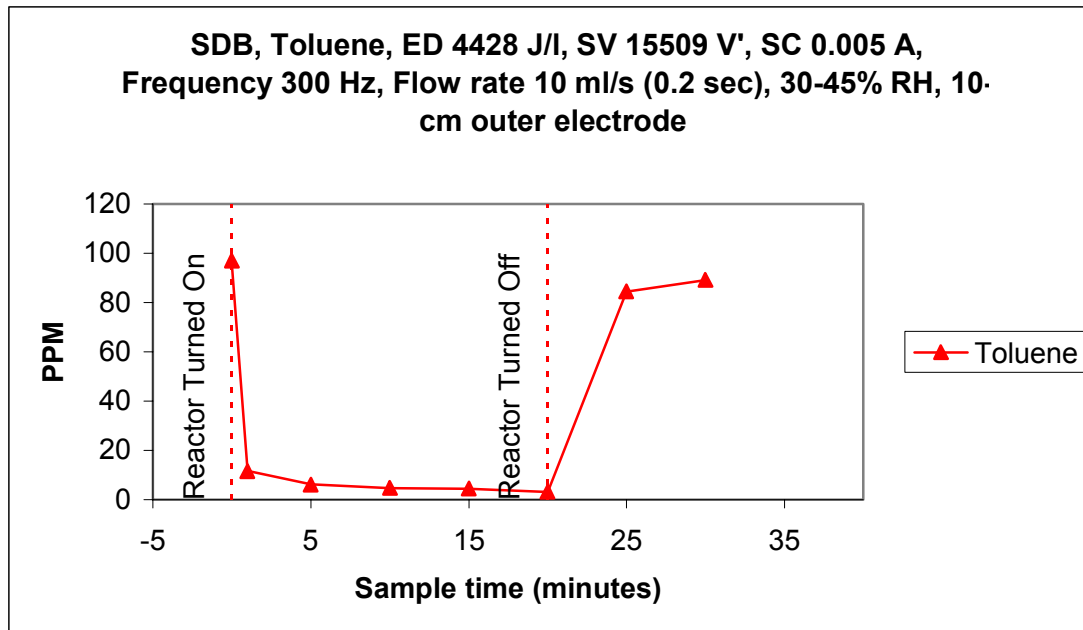


Figure 29: Destruction Run at 300 Hz Frequency

4.5. Effect of Flow Rate on Destruction

Three different flow rates were performed using this reactor: 6, 8, and 10 ml/s (0.33, 0.24, and 0.20 sec residence time respectively). Table 5 and Figures 30, 31, and, 32 shows the effect of flow rate, at constant 100 ppm toluene concentration, 30-45% relative humidity, 300 Hz frequency and secondary voltage of 15,000 V (approximately) on the destruction of toluene. The actual values of secondary voltage were 15,423, 15,136, and 15,374 V. Reynolds number was used to calculate the type of flow used in this study and the calculations were shown in Appendix I. In this study the flow was in laminar region.

From all of the runs conducted the results shows that increasing the flow rate decreased destruction of toluene.

Nunez et al. (1993) and Ahmad (1996) reported that an increase in flow rate (decrease in residence time) showed a decrease in destruction efficiency. Increase in flow rate will decrease the energy density as shown in equation 17. Korzekwa (1998) also showed that an increase in energy density above 95% DRE, negligible increased destruction efficiency (Table 5). Thus, destruction efficiency will be reduced.

Table 5: Effect of Flow Rate on Destruction of Toluene

| Flow Rate (ml/s) | Secondary Current (A) | Power Factor | Energy Density (J/l) | Influent Concentration (ppm) | Effluent Concentration at 20 min (ppm) | Destruction Efficiency (%) |
|------------------|-----------------------|--------------|----------------------|------------------------------|--|----------------------------|
| 10 | 0.004 | 0.574 | 3321 | 122.3 | 4.7 | 96.1 |
| 8 | 0.004 | 0.740 | 4210 | 87.1 | 2.8 | 96.7 |
| 6 | 0.003 | 0.862 | 7093 | 96.3 | 2.5 | 97.4 |

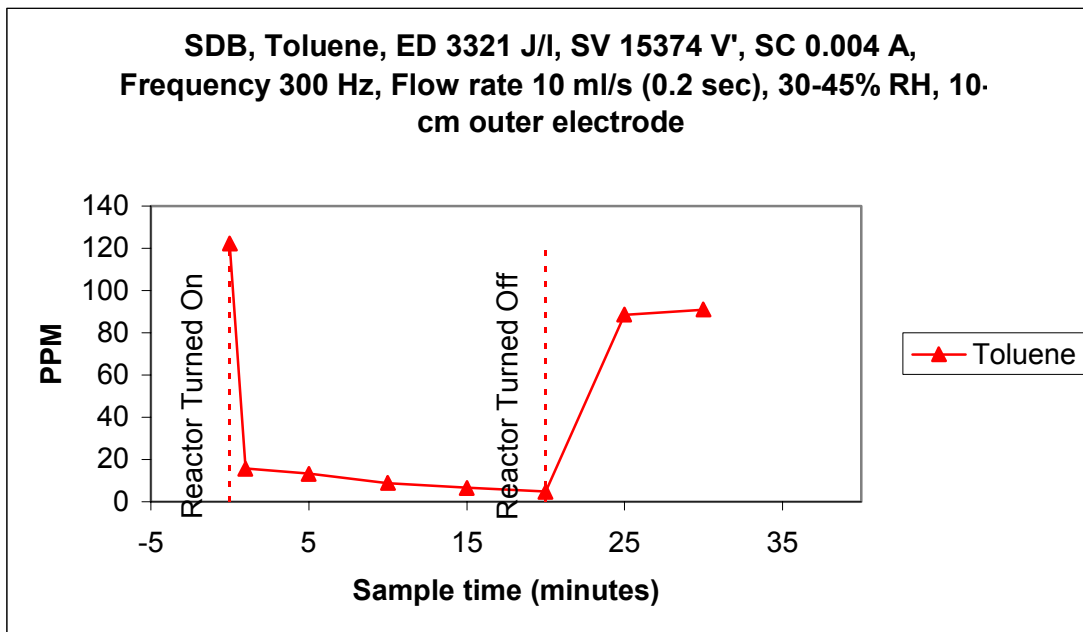


Figure 30: Destruction Run at 10 ml/s Flow Rate

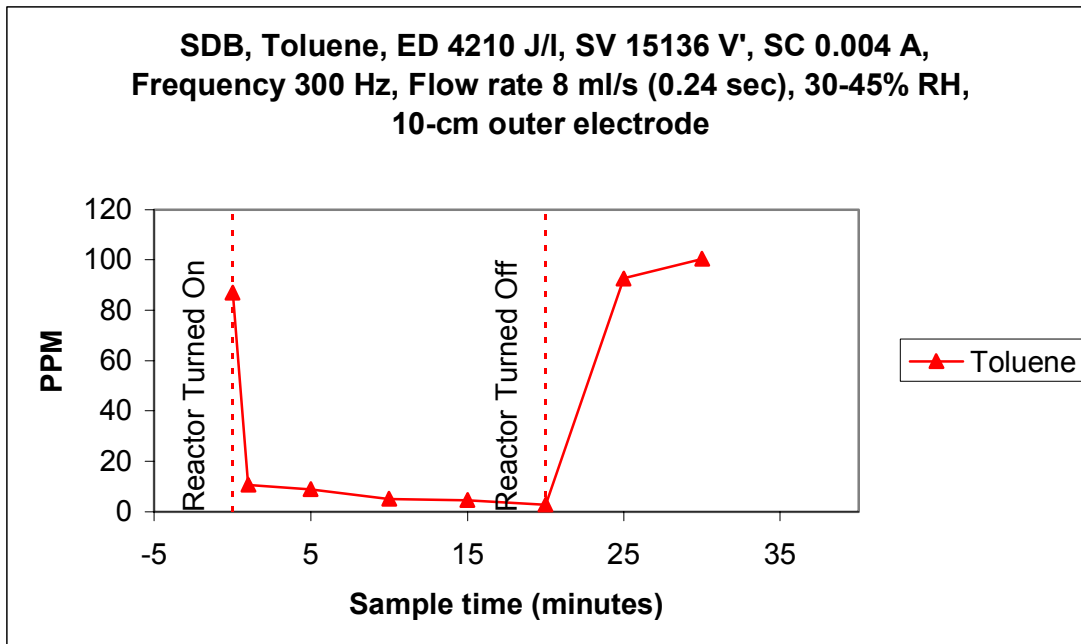


Figure 31: Destruction Run at 8 ml/s Flow Rate

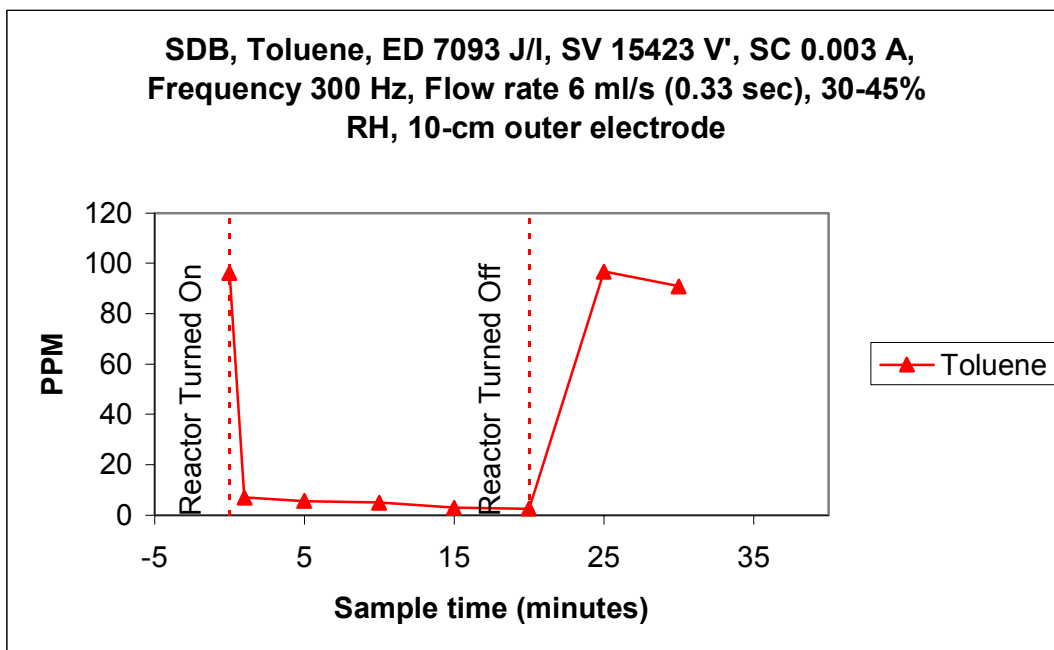


Figure 32: Destruction Run at 6 ml/s of Flow Rate

4.6. Effect of Energy Density on Destruction

The effect of energy density on the destruction of toluene was measured by using seven different energy density values. All the runs were conducted utilizing 100 ppm of toluene and 30-45 % RH. Table 6, and Figures 33, 34, 35, 36, 37, 38, and, 39 gives the detailed operating parameters used for this research.

Increasing energy density increased the destruction efficiency of toluene. This effect is shown in Table 5. A graph (Figure 40) was plotted between the energy density and destruction efficiency and fit through the origin in order to obtain information required to calculate a scale up parameter for toluene. The scale up parameter was calculated as 1233 J/L. This value was calculated from the slope of the line in the Figure 40. Yan (2001) reported scale up parameter toluene of 99 J/l. Thus the value obtained in this research is higher than Yan's (2001) calculated value. But, Korzekwa (1998) showed the same kind of fit (Figure 41) for the destruction of toluene vs. energy density above 95% DRE. Korzekwa data were replotted (Figure 40) and a scale up parameter for toluene was calculated as 368 J/l. Since most of the energy density in this work lies above the 95 % DRE and had the best fit line go through the origin gave higher value of 1233 J/l than the Yan (2001) and Korzekwa (1998) values.

Table 6: Effect of Energy Density on Destruction of Toluene

| Flow Rate (ml/s) | Frequency (Hz) | Actual Secondary voltage (V) | Secondary current (A) | Power factor | Energy Density (J/l) | Influent Concentration (ppm) | Effluent Concentration (ppm) at 20 min | Destruction Efficiency (%) |
|------------------|----------------|------------------------------|-----------------------|--------------|----------------------|------------------------------|--|----------------------------|
| 10 | 250 | 11452 | 0.002 | 0.61 | 1397 | 100.7 | 3.9 | 96.1 |
| 8 | 200 | 12044 | 0.002 | 0.72 | 2168 | 89.2 | 5.1 | 94.3 |
| 10 | 250 | 15649 | 0.003 | 0.71 | 3333 | 104.2 | 4.0 | 96.2 |
| 6 | 300 | 9076 | 0.003 | 0.80 | 3837 | 107.1 | 3.6 | 96.6 |
| 6* | 300* | 9429* | 0.004* | 0.65* | 4099* | 107.2* | 3.7* | 96.5* |
| 8 | 300 | 15136 | 0.004 | 0.74 | 4210 | 87.1 | 2.8 | 96.8 |
| 6 | 300 | 12337 | 0.004 | 0.78 | 6423 | 95.7 | 2.7 | 97.2 |
| 6 | 300 | 15423 | 0.003 | 0.86 | 7093 | 96.3 | 2.5 | 97.4 |

* Duplicate run of 300 Hz, 6 ml/s, 9076V SV, 0.003A SC

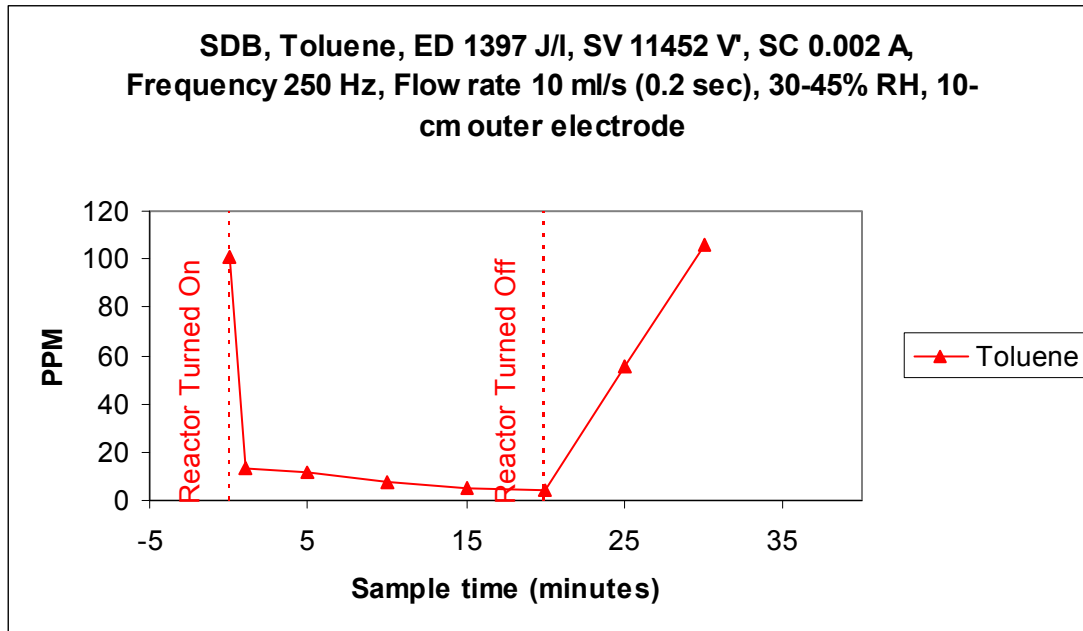


Figure 33: Destruction Run at 1397 J/l Energy Density

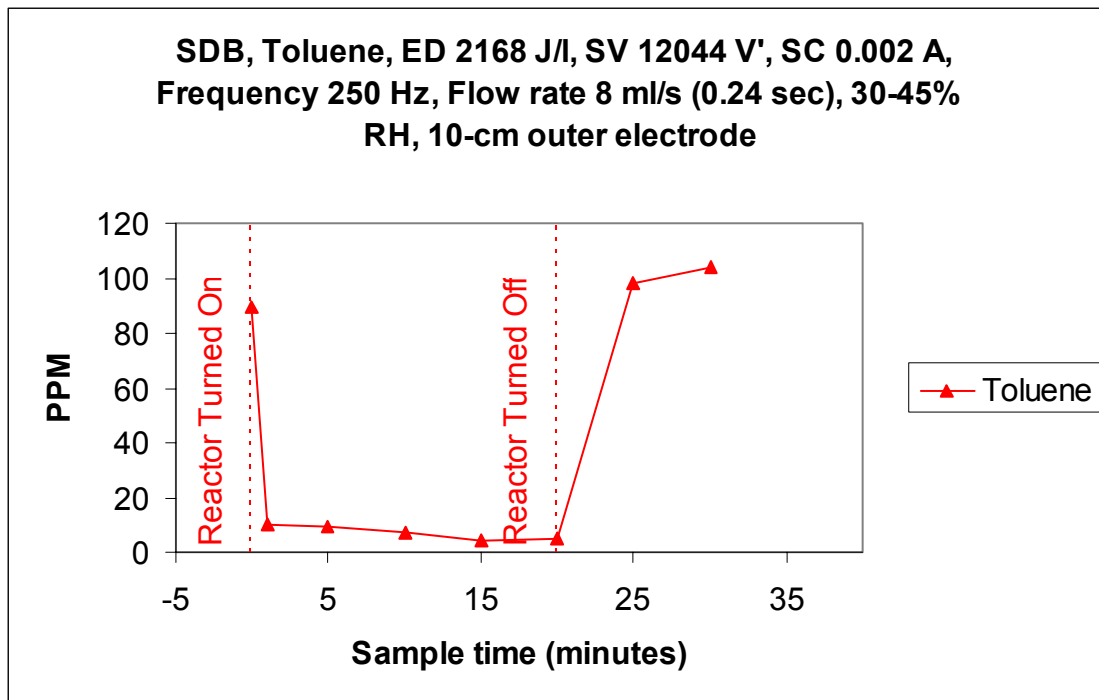


Figure 34: Destruction Run at 2168 J/l Energy Density

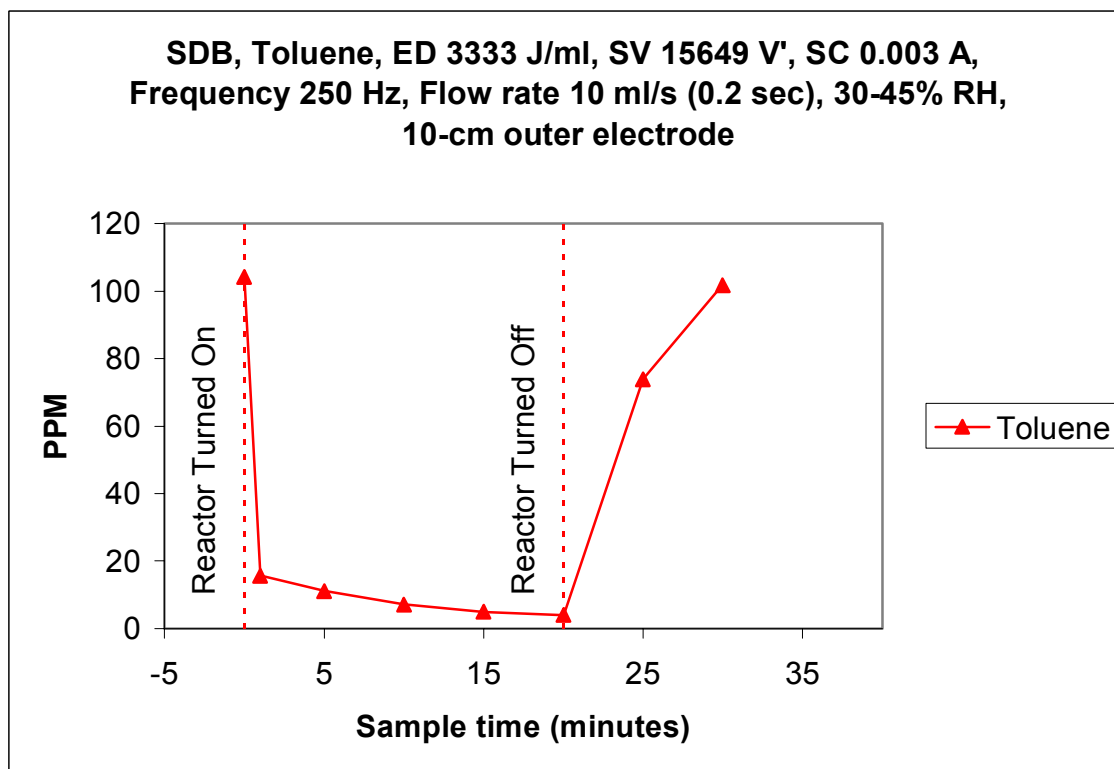


Figure 35: Destruction Run at 3333 J/l Energy Density

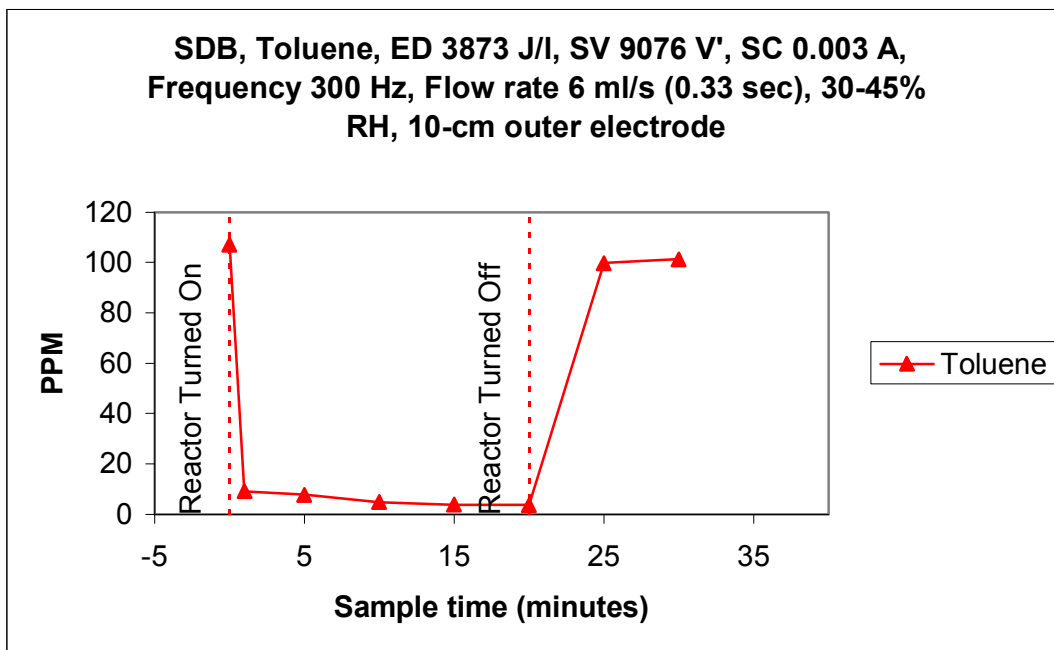


Figure 36: Destruction Run at 3873 J/l Energy Density

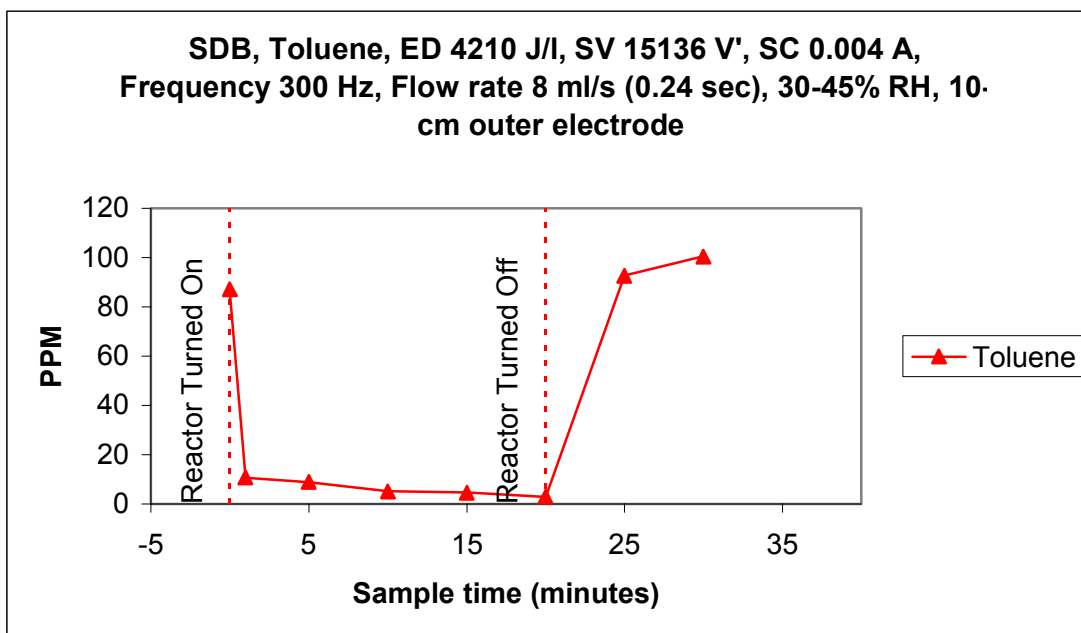


Figure 37: Destruction Run at 4210 J/l Energy Density

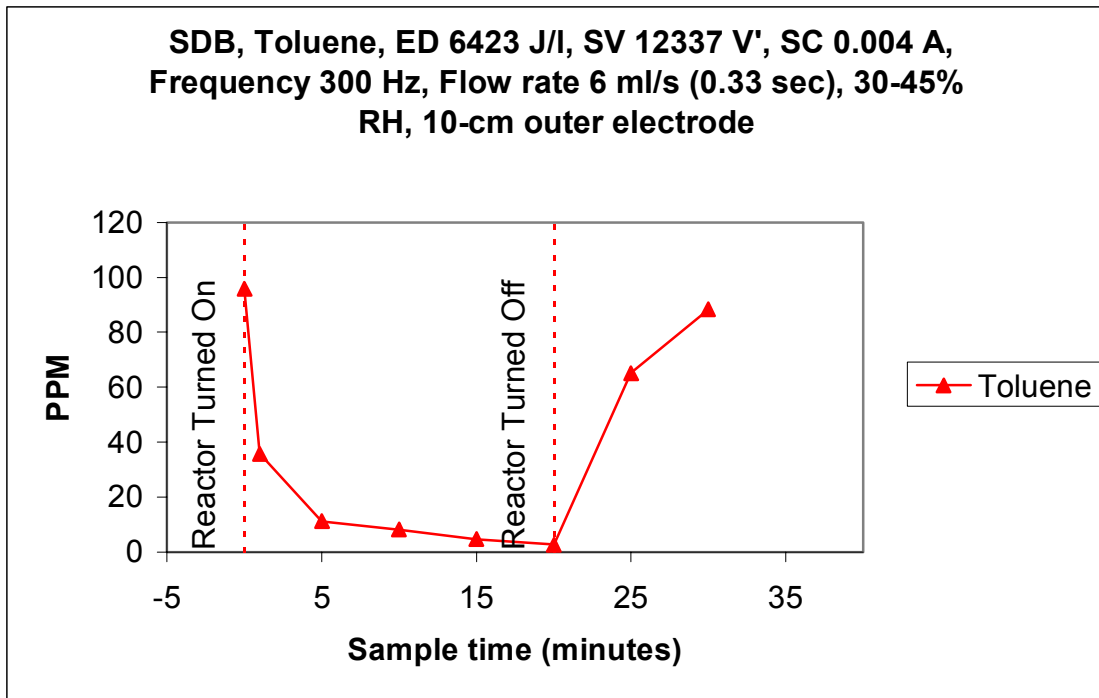


Figure 38: Destruction Run at 6423 J/l Energy Density

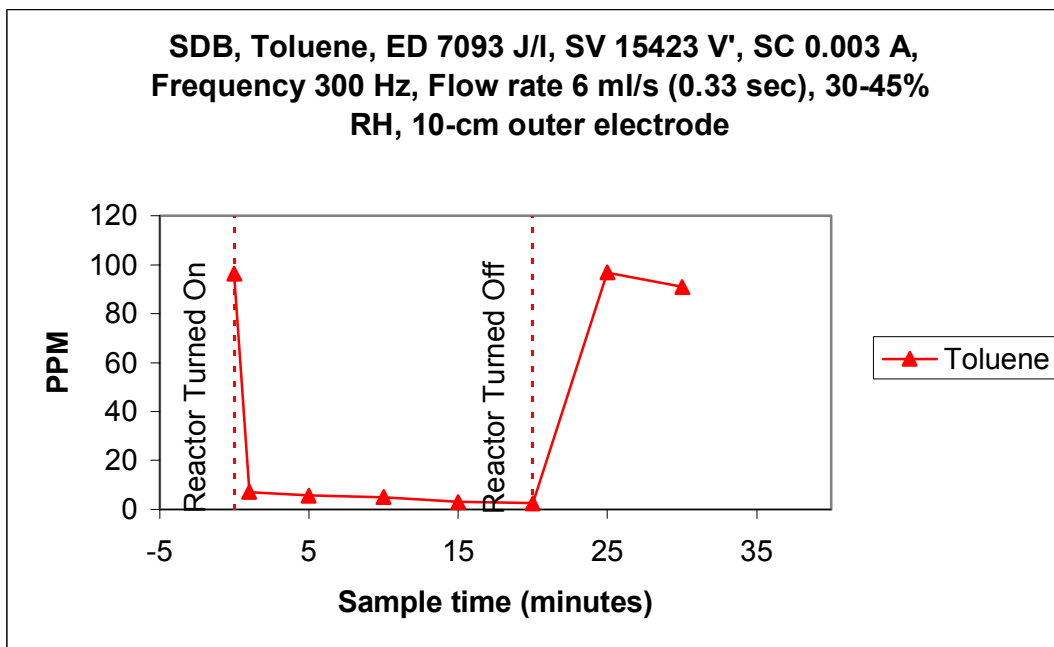


Figure 39: Destruction Run at 7093 J/l Energy Density

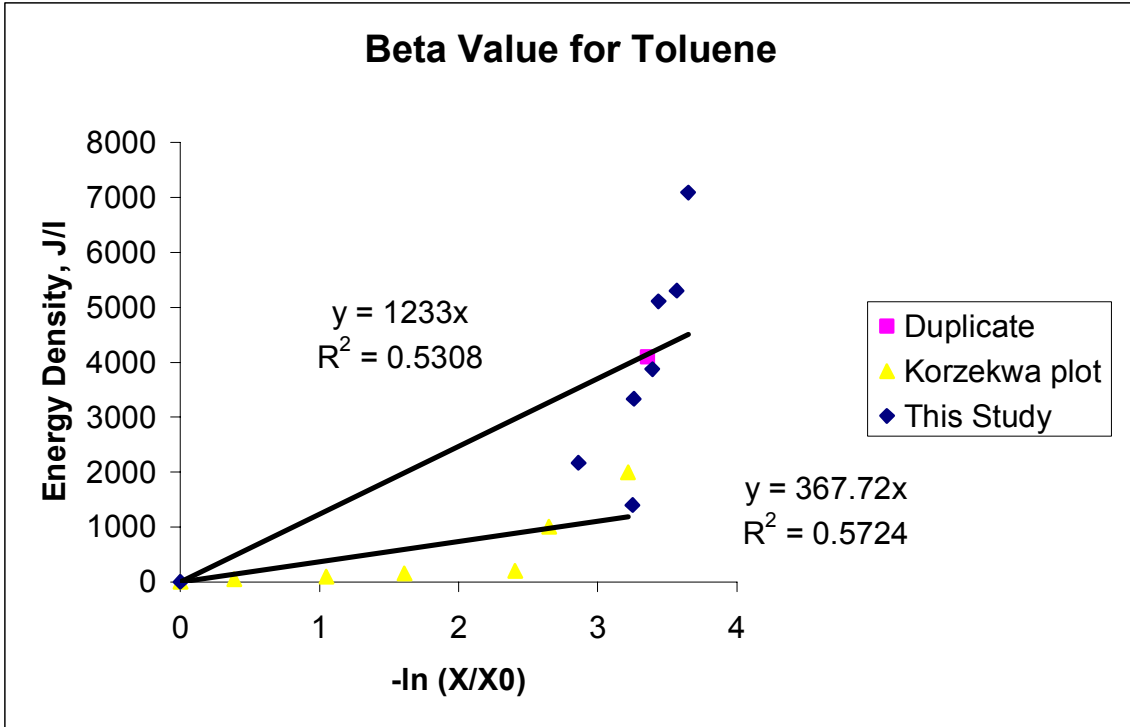


Figure 40: Scale up factor Calculation for Toluene

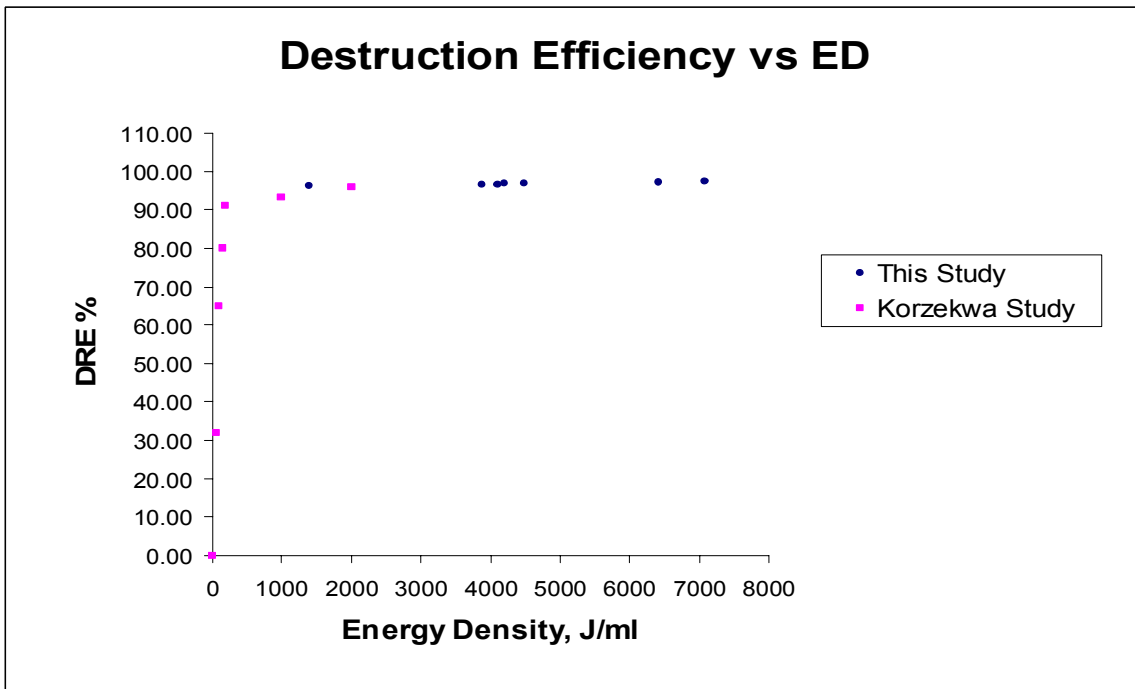


Figure 41: DRE vs. Energy Density

4.7. Carbon Balance

Overall carbon mass balances were calculated for the products entering and exiting the plasma reactor for various destruction runs utilizing 100 ppm of toluene. These were obtained by subtracting the total mass of carbon coming out of the reactor from the total mass of carbon entering. The mass balances for the reactor are given in the Table 7. The total mass of carbon coming in and out of the reactor over the 20 minute time (Figure 42) is plotted in the graph and integrated over the time. Since the CO and CO₂ are coming out at the same time in the GC, it was assumed that CO₂ was sole by-product in the calculation. The detailed calculation of the carbon balance is attached in Appendix J. There is enough oxygen (Appendix K) for the complete conversion of toluene into carbon dioxide.

The results indicate that more than 85% of carbon was accounted for almost all the runs, except the second one. The results also show that there is no definite pattern to the carbon balance when energy density was increased. Agnihotri (2003) reported carbon balance values of more than 70% in his runs.

Table 7: Carbon Balance of Toluene

| Energy density (J/l) | Mass of carbon at the inlet (g) | Mass of carbon at the outlet at 1 min (g) | Mass of carbon at the outlet at 5 min (g) | Mass of carbon at the outlet at 10 min (g) | Mass of carbon at the outlet at 15 min (g) | Mass of carbon at the outlet at 20 min (g) | Total mass of carbon at the inlet between 1 to 20 min (g) | Total mass of carbon at the outlet between 1 to 20 min (g) | % Carbon recovered |
|----------------------|---------------------------------|---|---|--|--|--|---|--|--------------------|
| 1397 | 2.0E-07 | 5.0E-08 | 3.1E-07 | 1.9E-07 | 2.0E-07 | 1.9E-07 | 4.0E-06 | 3.7E-06 | 92.5 |
| 2167 | 1.7E-07 | 5.9E-08 | 3.3E-07 | 3.5E-07 | 2.1E-07 | 2.0E-07 | 3.4E-06 | 3.6E-06 | 105.8 |
| 3333 | 2.1E-07 | 6.7E-08 | 2.6E-07 | 2.5E-07 | 1.6E-07 | 1.9E-07 | 4.2E-06 | 3.9E-06 | 92.9 |
| 3837 | 2.2E-07 | 5.5E-08 | 2.3E-07 | 2.0E-07 | 2.2E-07 | 2.1E-07 | 4.4E-06 | 4.0E-06 | 91.0 |
| 4210 | 1.7E-07 | 4.6E-08 | 1.7E-07 | 9.4E-08 | 1.6E-07 | 1.6E-07 | 3.4E-06 | 2.9E-06 | 85.3 |
| 6423 | 1.9E-07 | 8.0E-08 | 2.4E-07 | 2.4E-07 | 2.3E-07 | 1.8E-07 | 3.8E-06 | 3.7E-06 | 97.4 |
| 7093 | 1.9E-07 | 5.1E-08 | 1.8E-07 | 2.2E-07 | 1.8E-07 | 1.4E-07 | 3.8E-06 | 3.3E-06 | 86.8 |

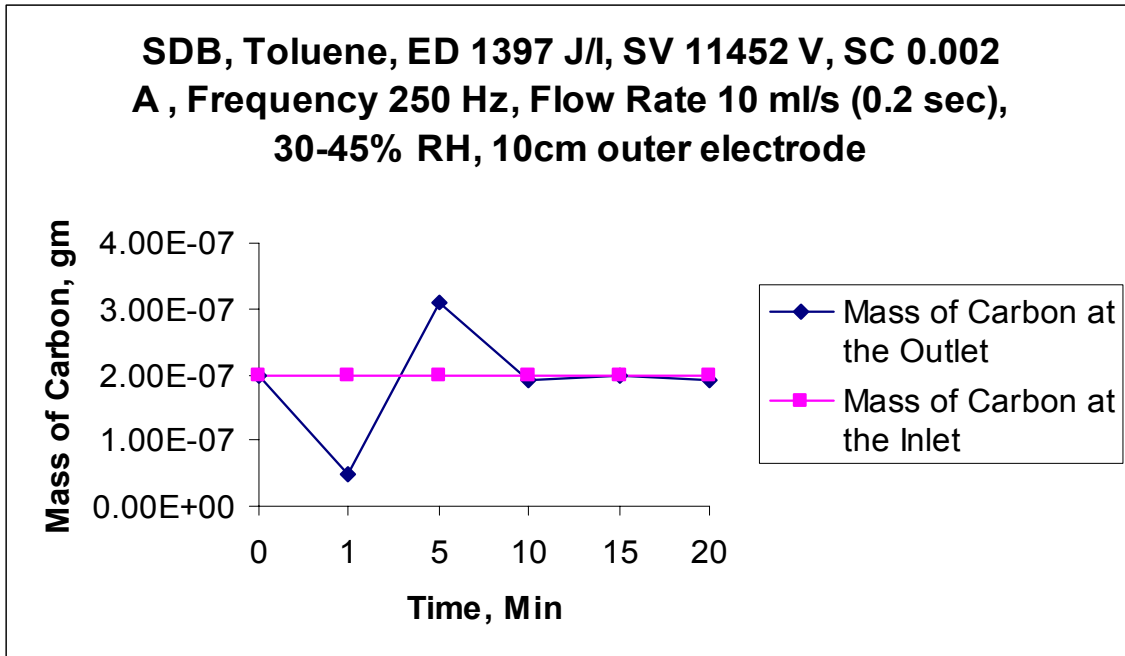


Figure 42: Carbon Balance Run 1

4.8. Repeatability

Figure 43 shows the values obtained when two tests were performed in the single tube single DBD reactor at the same settings (300 Hz, 6 ml/s, and 9000 theoretical secondary voltage) but on different days. The destruction efficiencies were 96.5% and 96.6% on the 1st and 2nd day, respectively. The overall fit is very good, showing excellent reproducibility. The lag in reaching the inlet concentration after the reactor was switched off is due to the retention time between the reactor and the outlet sampling port.

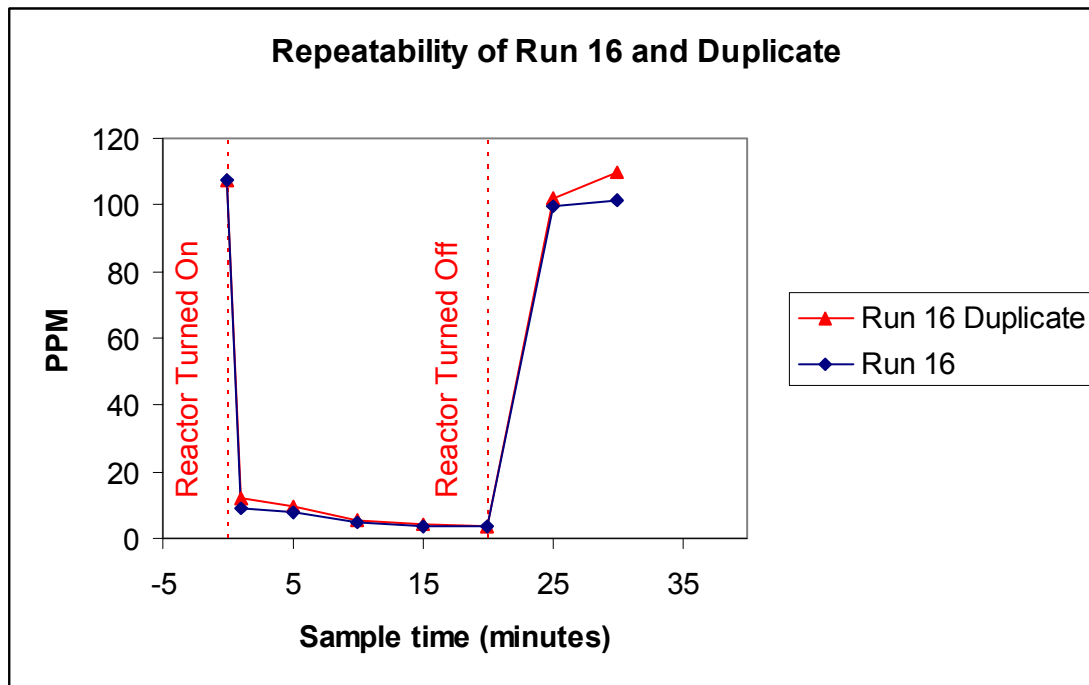


Figure 43: Repeatability of Run 16 and Duplicate

4.9. Cost Analysis

The total cost including capital and operational cost is calculated for the scaled up reactor, which has a flow rate of 1000 cfm and 100 ppm of toluene. The cost of transformer, oscillator, blower and sensors are costs supplied by the respective vendors. These costs include shipping and handling. A detailed capital cost is shown in Table 8.

The calculations show that it would take \$0.126 to treat 1000 cubic feet of air (100 ppm of toluene). A cost of 8.46 cents per kilowatt-hour (Firstgov, 2004) was assumed to calculate this operational cost. The detailed calculations are attached in Appendix L.

Table 8: Capital Cost

| UNIT | Quantity | Cost, \$ | Vendor |
|-----------------------------------|-------------------------|---------------|------------------------------------|
| Blower | 1(1000cfm) | 1,480 | Matches |
| Oscillator | 1 | 795 | California Instruments |
| Transformer | 278 | 33,304 | Jenkins Electric |
| Plasma reactor: | | | |
| Dielectric quartz tubes | 881 (10mm*12mm) | 22,906 | Technical Glass Products Inc |
| Inner electrode (stainless steel) | 881 (7.55' * 0.25 inch) | 6,960 | Small Parts Inc |
| Outer electrode (copper foil) | 100000cm(bundle) | 130 | McGills Warehouse |
| Fiberglass case for the reactor | 1 (20cm*110cm) | 150 | Niemiac Marine Inc |
| Vitan gaskets | 3 square feet | 132 | Scientific Instrument Services Inc |
| Piping: | | | Stillwater Steel Supply |
| 1. Carbon steel | | | |
| 16-10 inch RFSO 150# Flange | 1 | 744 | |
| 96-B7 Studs | 1 | 192 | |
| 8-10 inch Flex Gaskets | 1 | 68 | |
| 4-10 inch SK20 LR 90' s | 1 | 358 | |
| 40'-10' SK20 Pipe | 1 | 460 | |
| Electrical Cost | | | |
| Voltage divider | 1 | 8 | Radioshack |
| Optical isolators NTE3044 | 1 | 15 | Radioshack |
| Isolation amplifiers | 1 | 118 | Radioshack |
| Breadboard wires | 1 | 15 | Radioshack |
| 18AWG test lead wires | 1 | 8 | Radioshack |
| DAQ board PCI6023E | 1 | 395 | Radioshack |
| R6868 Ribbon Cable, 1m | 1 | 65 | Radioshack |
| CB-68LB I/O connector Block | 1 | 95 | Radioshack |
| LAB View software | 1 | 495 | National Instruments |
| 15V DC Power supply | | 395 | Radioshack |
| Sensors | | | All QA products |
| Temperature | 1 | 80 | |
| Pressure | 1 | 85 | |
| Humidity | 1 | 35 | |
| Power | 1 | 150 | |
| Voltage | 1 | 40 | |
| | Total Cost | 69,678 | |

5. Conclusions and Recommendations

5.1. Conclusions

The specific objectives of this research were to demonstrate that the plasma reactor was feasible for an instant-on and instant-off application, for the destruction of toluene and to calculate β , the scale up parameter for this compound.

- Increasing secondary voltage from 9000, 12,000, to 15,000, increased destruction efficiency (DRE) only with increase in energy density (Table 4), however the effect of energy density is small above 95% DRE.
- Increasing frequency from 200, 250 and 300 Hz, increased the destruction efficiency (Table 4) with the increase in energy density and again the effect of energy density is small above 95% DRE.
- Increasing flow rate 6, 8, and 10 ml/s decreased DRE (Table 5) with a decrease in energy density and its effect small above 95% DRE.
- Increasing energy density from 1397 to 7093 J/l, increased the destruction efficiency of toluene (Table 6), but the effect is negligible above 95% DRE.
- The scale up parameter β , for toluene was calculated as 1233 J/l (Figure 40). This value is higher than the Yan (2001) and Korzekwa (1998) Values of 99 and 367 J/l, respectively.
- An overall carbon balance of more than 85 % for toluene during destruction tested was observed (Table 7).
- From all the runs conducted (Table 2), the alternating current plasma reactor was proven to be an effective method of destruction for toluene (Tables 3, 4, 5, and 6) with instant-on and instant-off capabilities.

- Removal efficiencies in the range of 85- 96.9 % were observed for all the runs at constant 100 ppm toluene concentration and a relative humidity of 30-45% (Appendix H).

Considering the above results of the research, energy density seems to be a key variable in the destruction of toluene below 95% DRE and little effect above 95% DRE.

5.2. Recommendations

All of the research discussed above established groundwork for the use of a scale up parameter in the design of large scale operations. Recommendations for further research include the following:

- Further research needs to be performed for numerous VOCs to find the exact relationship between energy density and destruction efficiency of compounds. This will give the better picture of scale up parameter,
- Further research should be done for a more wider range of energy density values,
- Further research should be done to control energy density effectively,
- Further research to be done to find the effect of relative humidity on the destruction at constant energy density, and
- Further research should be carried out to figure the relationship between Gibbs free energy and the beta scale up parameter.

BIBLIOGRAPHY

1. Agnihotri S, and Cal M.P (2003), "Destruction of 1, 1, 1-trichloroethylene (TCA) using Non-Thermal Plasma (NTP)", Paper Presentation at Urbana, Illinois.
2. Ahmad I. (1993), "Destruction of Trichloroethylene and Toluene in an Alternate Current Plasma Reactor", MS Thesis, Oklahoma State University, Stillwater.
3. Cal, M.P., and Schluep. M. (2001), "Environmental Progress", 20 (3), pp:151-156.
4. Coogan, J.J., and Jassal, A.S. (1997), "Silent Discharge Plasma for Point of Use (POU) Abatement of Volatile Organic Compounds (VOC) Emissions: Final Report (ESH003)", SEMATECH Technology Transfer Document 97023244A-ENG.
5. Engineering Fundamentals (2004), "Properties of Air", Available:
http://www.efunda.com/materials/common_matl/show_gas.cfm?MatlName=Air0C
6. Glockler, G. , and S. C. Lind (1939), "The Electrochemistry of Gases and Other Dielectrics", John Wiley & Sons, Inc., New York.
7. Meek, J.M., and Craggs, J.D. (1953), "Electrical Breakdown of Gases", Wiley Interscience Publication, NY, pp 533-545.
8. Nunez, C.M.; Ramsey, G.H.; Ponder, W.H.; Abbot, J.H.; Hamel, L.E.; and Kariher,P.H. (1993), "Corona Destruction: An Innovative Control Technology for VOCs and Air Toxics", Journal of the Air & Waste Management Association 43 (2), pp: 242-247.

9. Plasma Science and Technology (2003), "What are Plasmas",
Available: <http://www.plasmas.org/rot-plasmas.htm>.
10. Pytte, A. (1990), "Clean Air Act Amendments", CQ, pp: 3934-3963.
11. Rosocha, L.A., and Korzekwa, R.A. (1996), "Advanced Oxidation and Reduction Processes in the Gas Phase Using Non-Thermal Plasmas", Journal of Advanced Oxidation Technologies, pp: 381-392.
12. Rosocha, L.A., Anderson, G.K, Bechtold, L.A., Coogan, J.J., Heck, H.G, Kang, M. McCulla, W.H, Tennant, R.A, and Wantuck, P.J. (1993), "Non-Thermal Plasma Techniques for Pollution Control", NATO ASI Series G: Ecological Sciences.G34-Pt B, pp: 281-306.
13. Rudolph, R, Francke, K.P, and Miessner, H. (2002), "Concentration Dependence of VOC Decomposition by Dielectric Barrier Discharges", Plasma Chemistry and Plasma Processing, Volume 22 (3), pp: 401-412.
14. Korzekwa, R.A, Grothaus, M.G, Hutcherson, R.K, Roush, R.A, and Brown, R (1998), "Destruction of Hazardous Air Pollutants using a Fast Rise Time Pulsed Corona Reactor", American Institute of Physics, Volume 69(4), pp 1886-1892.
15. SIRI MSDS Index (2003), "SIRI MSDS", Available: <http://hazard.com/msds/>
16. Unit Cost Estimator (2003), "NAVFAC", Available:
http://enviro.nfesc.navy.mil/erb/erb_a/restoration/technologies/sel_tools/tools/voc/Main/frMain.htm.
17. Veenstra J.N, (2003), " Gas Phase Corona Technology-Phase 1", Phase 1 Technical Report. Contract No. F34650-01-D-D703, D.O. 0008.

18. FirstGov (2004), "Electricity Quick Stats", Available:
<http://www.eia.doe.gov/neic/quickfacts/quickelectric.htm>
19. Yan, K, Van Heesch, E. J. M, Pemen, A. J. M, and Huijbrechts, P. A. H. J (2001),
"From Chemical Kinetics to Streamer Corona Reactor and Voltage Pulse
Generator", Plasma Chemistry and Plasma Processing, Volume 21(1), pp: 107-
137.

Appendix A

TABLE A1: 2001 AIR EMISSIONS INVENTORY, B2121 PAINT BOOTH

| CAS NO | CHEMICAL NAME | TONS/YEAR |
|-----------------|--|--------------|
| 64810-23-1 | POLYAMIDE RESIN | 0.182 |
| 107-87-9 | METHYL PROPYL KETONE | 0.117 |
| 4035-89-6 | 1,6-HEXAMETHYLENE DIISOCYANATE | 0.093 |
| 28182-81-2 | ALIPHATIC ISOCYANATE | 0.086 |
| 6/2/7789 | STRONTIUM CHROMATE | 0.077 |
| 64742-95-6 | AROMATIC HYDROCARBON | 0.071 |
| 78-92-2 | SEC-BUTYL ALCOHOL | 0.057 |
| 13463-67-7 | TITANIUM DIOXIDE | 0.055 |
| 763-69-9 | ETHYL 3-ETHOXYPROPIONATE | 0.054 |
| 123-86-4 | BUTYL ACETATE | 0.049 |
| 3779-63-3 | ALIPHATIC POLYISOCYANATE RESIN | 0.049 |
| 108-10-1 | METHYL ISOBUTYL KETONE | 0.045 |
| 110-43-0 | METHYL N-AMYL KETONE | 0.041 |
| 140-31-8 | ALIPHATIC AMINE | 0.031 |
| 108-941 | CYCLOHEXANONE | 0.025 |
| 1760-24-3 | AMINO SILANE ESTER | 0.015 |
| 78-93-3 | METHYL ETHYL KETONE | 0.015 |
| 90-72-2 | 2,4,6-TRIS(DIMETHYLAMINO METHYL) PHENOL | 0.015 |
| 108-88-3 | TOLUENE | 0.012 |
| 64742-48-9 | ALIPHATIC NAPHTHA | 0.012 |
| 123-54-6 | 2,4-PENTANEDIONE | 0.011 |
| 1330-20-7 | XYLENE | 0.01 |
| 64742-88-7 | MEDIUM ALIPHATIC NAPHTHA (AROMATIC 100) | 0.01 |
| 100-41-4 | ETHYL BENZENE | 0.007 |
| 127519-17-9 | BENZOTRIAZOLE DERIVATIVE | 0.005 |
| 41556-26-7 | BIS(1,2,2,6,6-PENTAMETHYL-4-PIPERIDINYL) SEPCATE | 0.005 |
| 64742-94-5 | HEAVY AROMATIC NAPHTHA | 0.005 |
| 64742-89-8 | LIGHT ALIPHATIC NAPHTHA | 0.003 |
| 67-64-1 | ACETONE | 0.003 |
| 95-63-5 | 1,2,4-TRIMETHYLBENZEN | 0.003 |
| 1119-40-4 | DIMETHYL GLUTARATE | 0.002 |
| 124-17-4 | DIETHYLENE GLYCOL MONOBUTYL ETHER ACETATE | 0.002 |
| 71-36-3 | N-BUTYL ALCOHOL | 0.001 |
| Particulates | | 0.011 |
| Organics | | 0.622 |
| VOC | | 0.447 |

APPENDIX B

TOLUENE

Physical and Chemical Properties

Appearance: Clear, colorless liquid.

Odor: Aromatic benzene-like.

Solubility: 0.05 gm/100gm water @ 20C (68F).

Specific Gravity: 0.86 @ 20C / 4 C

pH: No information found.

% Volatiles by volume @ 21C (70F): 100

Boiling Point: 111C (232F)

Melting Point: -95C (-139F)

Vapor Density (Air=1): 3.14

Vapor Pressure (mm Hg): 22 @ 20C (68F)

Evaporation Rate (BuAc=1): 2.24

Stability and Reactivity

Stability: Stable under ordinary conditions of use and storage. Containers may burst when heated.

Hazardous Decomposition Products: Carbon dioxide and carbon monoxide may form when heated to decomposition.

Hazardous Polymerization: Will not occur.

Incompatibilities: Heat, flame, strong oxidizers, nitric and sulfuric acids, chlorine, nitrogen tetroxide; will attack some forms of plastics, rubber, coatings.

Conditions to Avoid: Heat, flames, ignition sources and incompatibles.

Toxicological Information

Toxicological Data: Oral rat LD50: 636 mg/kg; skin rabbit LD50: 14100 uL/kg; inhalation rat LC50: 49 gm/m³/4H; Irritation data: skin rabbit, 500 mg, Moderate; eye rabbit, 2 mg/24H, Severe. Investigated as a tumorigen, mutagen, reproductive effectors.

Reproductive Toxicity: Has shown some evidence of reproductive effects in laboratory animals.

-----\Cancer Lists\-----

---NTP Carcinogen---

| Ingredient | Known | Anticipated | IARC Category |
|--------------------|-------|-------------|---------------|
| Toluene (108-88-3) | No | No | 3 |

Ecological Information

Environmental Fate:

When released into the soil, this material may evaporate to a moderate extent. When released into the soil, this material is expected to leach into groundwater. When released into the soil, this material may biodegrade to a moderate extent. When released into water, this material may evaporate to a moderate extent. When released into water, this material may biodegrade to a moderate extent. When released into the air, this material may be moderately degraded by reaction with photo chemically produced hydroxyl radicals. When released into the air, this material is expected to have a half-life of less than 1 day. This material is not expected to significantly bioaccumulate. This material has a log octanol-water partition coefficient of less than 3.0. Bioconcentration factor = 13.2 (eels).

Environmental Toxicity:

The LC50/96-hour values for fish are between 10 and 100 mg/l (SIRI MSDS, 2003).

In human beings the primary effect is on the central nervous system. Single short-term exposure toluene (750 mg/m³ for 8 hours) has reportedly caused transient eye and respiratory irritation. Repeated long-term exposure in this range can cause neurological damage. (WHO, 1985)

Appendix C

Injection volume determination for Toluene

Determine the volume of toluene to be used for 100 ppm concentration:

T= 298 K

1 mole of any substance occupies 22,400 ml

Therefore x ml/min of air contains = x ml/min / 22400 ml/mole

$$\text{Injection Rate} = \frac{\text{Required ppm} * \text{Flow rate of air (ml/min)} * \text{Molecular Weight (g/mole)}}{\text{Density (g/ml)} * 22400 \text{ (ml/mole)} * 1\text{E}6}$$

Diameter of Syringe = 7.28 mm

Volume of syringe = 2.5 ml

The various injection rates for toluene are given in the following Table C1

Table C1: Injection rate of toluene

| Concentration (ppm) | Flow rate of air (ml/min) | Injection Rate (ul/min) |
|----------------------------|----------------------------------|--------------------------------|
| 100 | 600 | 0.29 |
| 100 | 480 | 0.23 |
| 100 | 360 | 0.17 |

Appendix D

Table D1: Mass Flow Controller Calibration Data

| Reading | Flow rate (ml/min) |
|----------------|---------------------------|
| 10 | 48 |
| 25 | 59 |
| 40 | 70 |
| 65 | 87 |
| 80 | 97 |
| 100 | 111 |
| 125 | 130 |
| 150 | 148 |
| 175 | 165 |
| 200 | 185 |
| 225 | 202 |
| 251 | 217 |
| 275 | 235 |
| 300 | 252 |
| 325 | 267 |
| 350 | 285 |
| 375 | 302 |
| 401 | 318 |
| 426 | 335 |
| 451 | 353 |
| 476 | 372 |
| 502 | 390 |
| 526 | 407 |
| 551 | 423 |
| 576 | 439 |
| 601 | 455 |
| 625 | 472 |
| 651 | 489 |
| 677 | 508 |
| 701 | 526 |
| 727 | 547 |
| 751 | 567 |
| 777 | 591 |
| 802 | 610 |
| 827 | 629 |
| 852 | 648 |
| 876 | 665 |
| 902 | 677 |
| 927 | 703 |
| 952 | 717 |
| 976 | 732 |

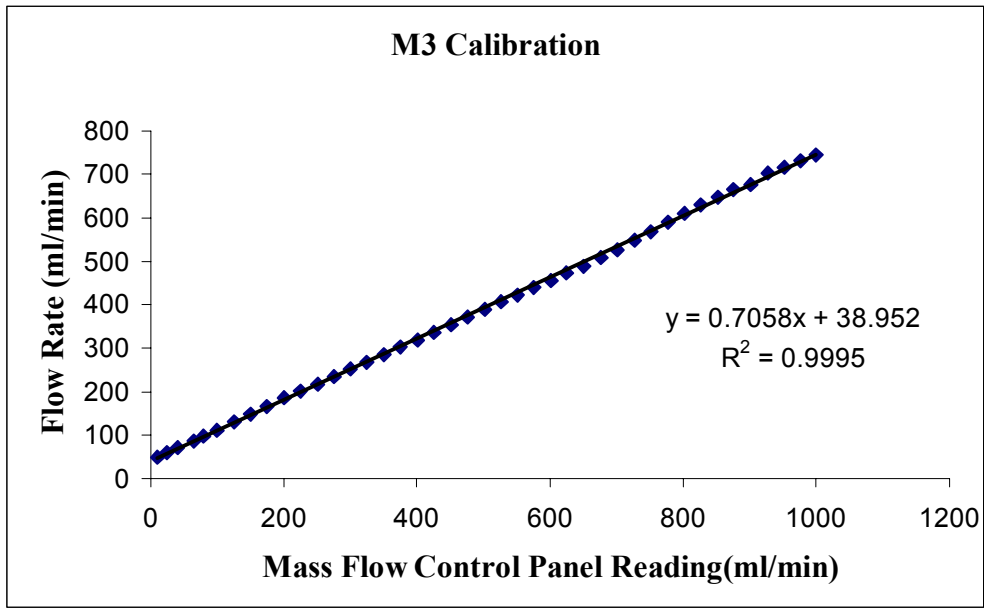


Figure D1: M3 Calibration

Appendix E

Table E1: Rotameter Calibration

| Height | Flow Rate, ml/min |
|--------|-------------------|
| 8 | 178 |
| 10 | 490 |
| 15 | 1280 |
| 20 | 1800 |
| 35 | 4500 |
| 60 | 8100 |
| 90 | 12812 |

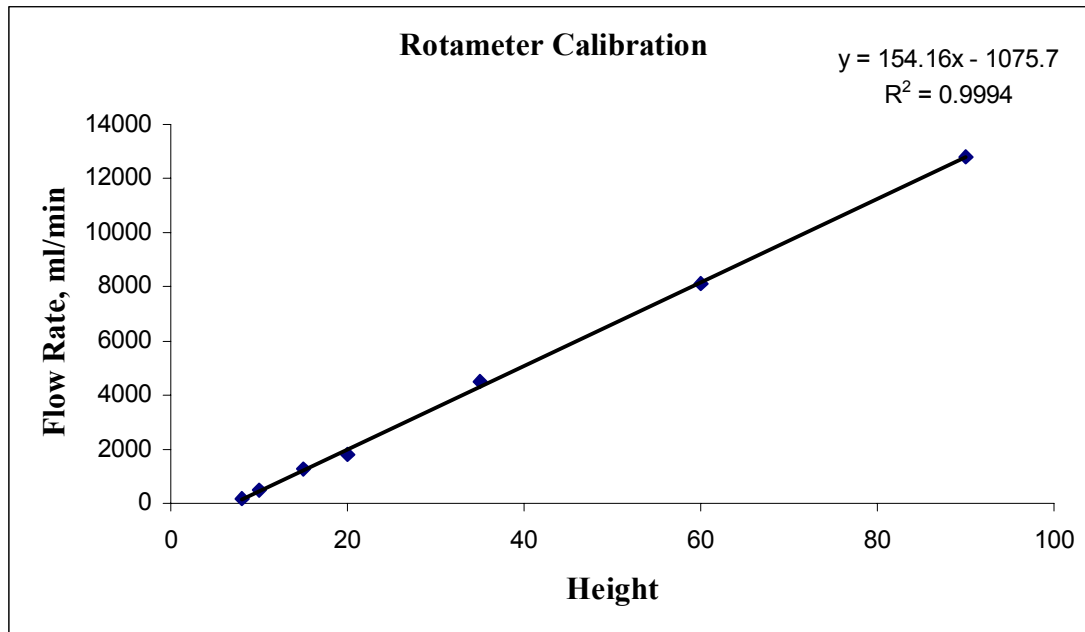


Figure E1: Rotameter Calibration

Appendix F

Calculation of mass from the calibration

$$N = PV / RT$$

V= volume of sample

P= 1 atm

R= 0.08206 L-atm/mole-K

T=298 K

n= number of moles compound

$$\text{Mass of sample} = (n * \text{ppm} * \text{Molecular weight}) / 1E6)$$

Appendix G

Table G1: Calibration Data for toluene

| Injection volume (mL) | Mass, g | Average Area |
|------------------------------|----------------|---------------------|
| 0.1 | 4.3E-08 | 272 |
| 0.2 | 8.6E-08 | 594 |
| 0.3 | 1.3E-07 | 1040 |
| 0.4 | 1.7E-07 | 1432 |
| 0.5 | 2.2E-07 | 1739 |
| 0.6 | 2.6E-07 | 2208 |
| 0.7 | 3.0E-07 | 2691 |

Table G2: CO calibration data

| Injection volume (ml) | Mass, g | Average Area |
|------------------------------|----------------|---------------------|
| 0.1 | 5.7E-08 | 356 |
| 0.2 | 1.1E-07 | 660 |
| 0.3 | 1.7E-07 | 970 |
| 0.4 | 2.3E-07 | 1313 |
| 0.5 | 2.9E-07 | 1625 |
| 0.6 | 3.4E-07 | 1993 |
| 0.7 | 4.0E-07 | 2328 |
| 0.8 | 4.6E-07 | 2612 |
| 0.9 | 5.1E-07 | 2919 |
| 1.0 | 5.7E-07 | 3255 |
| 1.3 | 7.2E-07 | 3900 |
| 1.8 | 1.0E-06 | 5419 |
| 2.0 | 1.1E-06 | 6245 |

Table G3: CO₂ Calibration data

| Injection Volume, ml | Mass, g | Average Area |
|-----------------------------|----------------|---------------------|
| 0.1 | 9.4E-08 | 318 |
| 0.2 | 1.9E-07 | 639 |
| 0.3 | 2.8E-07 | 969 |
| 0.4 | 3.7E-07 | 1309 |
| 0.5 | 4.7E-07 | 1684 |
| 0.6 | 5.6E-07 | 2015 |
| 0.7 | 6.5E-07 | 2366 |
| 0.8 | 7.5E-07 | 2695 |
| 0.9 | 8.4E-07 | 3003 |
| 1.0 | 9.4E-07 | 3394 |
| 1.2 | 1.7E-06 | 4214 |
| 1.7 | 1.6E-06 | 5357 |
| 2.0 | 1.7E-06 | 6085 |

Appendix H

Table H1: Actual Operating Conditions

| Run | Influent | Effluent at 20 min | Efficiency, % | Secondary Voltage (V) | Secondary Current (A) | Power Factor | Flow Rate, ml/s | Reynolds Number | Energy Density, J/l |
|------------|-----------------|---------------------------|----------------------|------------------------------|------------------------------|---------------------|------------------------|------------------------|----------------------------|
| 1 | 97.1 | 3.1 | 96.8 | 15509 | 0.005 | 0.571 | 10 | 163 | 4428 |
| 1 Dup | 122.3 | 4.7 | 96.2 | 15374 | 0.004 | 0.574 | 10 | 163 | 3321 |
| 2 | 124.4 | 3.3 | 97.3 | 12414 | 0.006 | 0.862 | 10 | 163 | 6421 |
| 2 Dup | 116.6 | 11.7 | 90.0 | 12332 | 0.003 | 0.726 | 10 | 163 | 2686 |
| 3 | 79.4 | 2.7 | 96.6 | 9251 | 0.006 | 0.705 | 10 | 163 | 3904 |
| 4 | 97.1 | 3.1 | 96.8 | 15509 | 0.005 | 0.571 | 10 | 163 | 4428 |
| 5 | 104.2 | 4.0 | 96.2 | 15649 | 0.003 | 0.710 | 10 | 163 | 3333 |
| 6 | 119.6 | 16.8 | 86.0 | 15203 | 0.002 | 0.650 | 8 | 131 | 2470 |
| 7 | 97.1 | 3.1 | 96.8 | 15509 | 0.005 | 0.571 | 10 | 163 | 4428 |
| 8 | 87.1 | 2.8 | 96.8 | 15136 | 0.004 | 0.740 | 8 | 131 | 4210 |
| 9 | 96.3 | 2.5 | 97.4 | 15423 | 0.003 | 0.862 | 6 | 98 | 7093 |
| 9 Dup | 105.9 | 3.3 | 96.9 | 15109 | 0.003 | 0.594 | 6 | 98 | 4487 |
| 10 | 100.7 | 3.9 | 96.1 | 11452 | 0.002 | 0.610 | 10 | 163 | 1397 |
| 11 | 104.2 | 4.0 | 96.2 | 15649 | 0.003 | 0.710 | 10 | 163 | 3333 |
| 12 | 89.2 | 5.1 | 94.3 | 12044 | 0.002 | 0.72 | 8 | 131 | 2168 |
| 13 | 87.1 | 2.8 | 96.8 | 15136 | 0.004 | 0.740 | 8 | 131 | 4210 |
| 14 | 96.3 | 2.5 | 97.4 | 15423 | 0.003 | 0.862 | 6 | 98 | 7093 |
| 14 Dup | 105.9 | 3.3 | 96.9 | 15109 | 0.003 | 0.594 | 6 | 98 | 4487 |
| 15 | 95.7 | 2.7 | 97.2 | 12337 | 0.004 | 0.781 | 6 | 98 | 6423 |
| 16 | 107.2 | 3.7 | 96.5 | 9429 | 0.004 | 0.652 | 6 | 98 | 4098 |
| 16 Dup | 107.1 | 3.6 | 96.6 | 9076 | 0.003 | 0.810 | 6 | 98 | 3873 |

Energy Density Calculation

Energy density = (Secondary voltage * Secondary Current* power factor)/flow rate

For the 1st run

$$\begin{aligned} \text{ED} &= 15509 \text{ V} * 0.005 \text{ A} * 0.571 / 10 \text{ ml/s} \\ &= 4428 \text{ J/l} \end{aligned}$$

Appendix I

Reynolds Number Calculation

Re= velocity* Diameter of Pipe/ Kinematic Viscosity (Engineering Fundamentals, 2004)

Kinematic Viscosity at 25° C = 1.56E-05 m²/s (Engineering Fundamentals, 2004)

Diameter of pipe = 0.005 m

For 10 ml/s (0.509 m/s)

$$= 0.509 \text{ m/s} * 0.005 / 1.56\text{E-}05$$

$$= 163$$

For 8 ml/s (0.407 m/s)

$$=131$$

For 6 ml/s (0.305 m/s)

$$= 98$$

Appendix J

Carbon Balance

Calculation is done for 1397 J/l energy density

Mass of Carbon at the Inlet:

Area of the toluene at the inlet = 2030

Total mass of toluene at the inlet (from calibration) = $2.2E-07$ gm

$$(y=1E-07X+2E-07)$$

Molecular weight of toluene = 92 gm/gmmole

92 gm of toluene has 84 gm of carbons

Total mass of carbon at the inlet = $2.2E-7$ gm of toluene * 84 gm of carbon /

92 gm of toluene

= $2.0E-7$ gm of carbon

Mass of Carbon at the Outlet :

The mass of carbon coming out of the reactor at 1, 5, 10, 15 and 20 min were calculated (a sample of 20 min calculation is as follows)

Toluene:

Area of the toluene at the outlet = 49

Total mass of toluene at the outlet = $2.5E-8$ gm

Total mass of carbons at the outlet = $2.3E-8$ gm

CO₂/CO:

Assume all the carbon atoms are converted to CO₂

Area of the CO₂ at the outlet = 2135

Mass of CO₂ (from calibration) = $2.9E-10$ * area

$$= 6.2E-7 \text{ gm}$$

44 gm of CO₂ has 12 gm of carbon

$$\text{Mass of carbon at the outlet} = 1.7E-7 \text{ gm}$$

$$\begin{aligned} \text{Total mass of carbon at the outlet} &= \text{Mass of carbon from toluene} + \text{Mass} \\ &\quad \text{of carbon from CO}_2 \end{aligned}$$

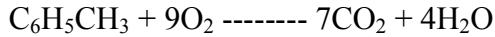
$$= 2.3E-8 + 1.7E-7$$

$$= 1.9E-7 \text{ gm}$$

Thus, the calculated mass of carbon were plotted in the graph (Figure 42) and integrated over the 1 to 20 min time.

Appendix K

Calculation of Oxygen Requirements for Toluene



1 gmmole of toluene requires 9 moles of oxygen

1 gmmole of any substance occupies 24.5 lit at 1 atm pressure, and 298 K

Table K1: Injection rate of toluene

| Concentration (ppm) | Flow rate of air (ml/min) | Injection Rate (ul/min) |
|---------------------|---------------------------|-------------------------|
| 100 | 600 | 0.29 |
| 100 | 480 | 0.23 |
| 100 | 360 | 0.17 |

600 ml of air contains 0.024 gmmole of air

Air contains 20.9% oxygen and 79.1% nitrogen by volume

Therefore 0.024 gmmole of air contains 5.04E-03 gmmole of oxygen

2.9E-07 ml of toluene contains 1.18E-08 gmmole of toluene

Therefore oxygen required = 9 gmmole of oxygen* 1.18E-08 gmmole of toluene/1 gmmole of toluene
= 1.06E-07 gmmole of oxygen (less than the available 5.04E-03 gmmole oxygen)

Appendix L

Operating Cost

Assume optimum Energy density $1.5 \text{ J/ml} = 1.5 \text{ watt-s/ml}$

Total flow = $1000 \text{ cfm} = 60,000 \text{ cubic feet/hr}$
 $= 1.5 \text{ kw-hr/1000 cubic feet}$

Assume $\$0.0846/\text{kw-hr}$

Operational cost = $(1.5 \text{ kw-hr} * 0.0846) / 1000 \text{ cubic feet}$

$= \$0.126/1000 \text{ cubic feet}$

VITA

Elangovan Karuppasamy

Candidate for the Degree of Master of Science

Thesis: DESTRUCTION OF TOLUENE IN A DIELECTRIC BARRIER
DISCHARGE PLASMA REACTOR

Major Field: Environmental Engineering

Personal Data: Born in Ottapidaram, India, June 2, 1980;
the son of Karuppasamy and Thamizharasi

Education: John the Baptist Higher Secondary School - May 1995

Bachelor of Science degree in Chemical Engineering, from University of Madras;
Chennai, India - May 2002

Completed the requirements for the Master of Science degree with a major in
Environmental Engineering at Oklahoma State University - December 2004

Experience: Worked for Oklahoma State University as a *Teaching Assistant* and
Research Assistant from 2002 to 2004.

Professional

Memberships: Indian Institute of Chemical Engineers

Chi Epsilon

Name: Elangovan Karuppasamy

Date of Degree: December, 2004

Institution: Oklahoma State University

Location: Stillwater, Oklahoma

Title of Study: DESTRUCTION OF TOLUENE IN A DIELECTRIC BARRIER
DISCHARGE PLASMA REACTOR

Pages in Study: 94

Candidate for the Degree of Master of Science

Major Field: Environmental Engineering

Scope and Method of Study: The purpose of this study was to determine the feasibility of a Single Tube Single Dielectric Barrier Discharge (DBD) Plasma Reactor for destruction of toluene in the air phase and to find β , a scale up parameter. The chief area of interest was the relationships between energy density and destruction efficiency. A number of process variables were examined including secondary voltage, frequency, flow rate and energy density.

Findings and Conclusions: Removal efficiencies for toluene in the range of 85-96.9 % were observed at relative humidity of 30-45%. Increasing energy density increased the destruction efficiency at a constant inlet concentration and relative humidity. Also, a carbon balance of more than 85 % was obtained for toluene during destruction testing. The calculated β value for toluene was 1233 J/L and this value is higher than the literature value of 99 J/L.

Advisor's Approval: _____